NASA TECHNICAL NOTE

NASA TN D-3670

NASA TN D-3670

COMPARISON OF CALCULATED AND MEASURED CHARACTERISTICS OF HORIZONTAL MULTITUBE HEAT EXCHANGER WITH STEAM CONDENSING INSIDE TUBES

by Harold H. Coe, Orlando A. Gutierrez, and David B. Fenn

Lewis Research Center
Cleveland, Ohio

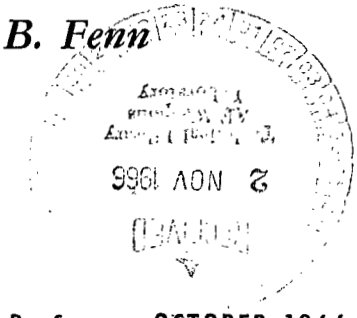

NATIONAL AERONAUTICS AND SPACE ADMINISTRATION • WASHINGTON, D. C. • OCTOBER 1966

NASA TN D-3670

COMPARISON OF CALCULATED AND MEASURED CHARACTERISTICS OF HORIZONTAL MULTITUBE HEAT EXCHANGER WITH STEAM CONDENSING INSIDE TUBES

By Harold H. Coe, Orlando A. Gutierrez, and David B. Fenn

Lewis Research Center
Cleveland, Ohio

NATIONAL AERONAUTICS AND SPACE ADMINISTRATION

For sale by the Clearinghouse for Federal Scientific and Technical Information
Springfield, Virginia 22151 – Price $2.00

COMPARISON OF CALCULATED AND MEASURED CHARACTERISTICS OF HORIZONTAL MULTITUBE HEAT EXCHANGER WITH STEAM CONDENSING INSIDE TUBES

by Harold H. Coe, Orlando A. Gutierrez, and David B. Fenn

Lewis Research Center

SUMMARY

As part of an overall research program of Rankine space power systems, a test facility using water as the working fluid was constructed. One of the purposes of this facility was to obtain experimental data on a convectively cooled, shell-and-tube condenser and to compare the resulting values with predicted values. Measured values of the overall heat-transfer coefficient, the condensing length, and the overall pressure drop were determined over a range of condenser inlet pressures of 8 to 30 pounds per square inch absolute and vapor qualities of 40 to 100 percent with tube inlet vapor Reynolds numbers of 13 000 to 44 000. The experimental condensing data were taken with a constant coolant flow rate in the shell and with two set values of coolant inlet temperature.

The predicted overall coefficients and condensing lengths were calculated by using conventional correlations and equations. The predicted overall pressure drops included a calculation for the two-phase friction pressure drop that utilized an approximating equation (derived in this report) based on the correlation of Lockhart and Martinelli.

Comparisons between the calculated and measured results were presented over a range of overall coefficients from 450 to 650 Btu per hour per square foot per ^{o}F, condensing lengths from 10 to 110 inches, and overall pressure drops from 0.2 to 9 pounds per square inch. The predicted values of the overall coefficient and condensing length were within ±20 percent of the measured values. The predicted pressure drops were within 50 to -20 percent of the measured data, with the largest deviations at the smaller pressure drops.

INTRODUCTION

Considerable interest has been shown in the Rankine cycle turbogenerator system as a source of electrical power in space (ref. 1). In this system, a heat source, such as a nuclear reactor, is used to boil a working fluid. The vapor thus produced drives a turbine, and the turbine drives the generator which produces the electric power. The turbine exhaust vapor is then condensed and the working fluid returned to the boiler to complete the cycle.

To develop such a system, it became evident that more information was needed on the performance of a complete power system and on the behavior of the individual components. Likewise, it was important to determine how well the performance of these components could be predicted with existing correlations and theories.

As part of the research program at the NASA Lewis Research Center of Rankine space power systems, a test facility using water as the working fluid was constructed (ref. 2) as a model of a similar alkali metal facility. The purpose of this water facility was to investigate the steady-state performance of a convectively cooled condenser system and to obtain a comparison of experimental data with predicted performance of the condenser. Results describing the operating characteristics of the complete system are presented in reference 2, and the results of an analysis of the condenser data are contained herein.

The condenser was a shell-and-tube heat exchanger with the water vapor condensing inside the tubes. It was fabricated with small diameter tubes and was installed in a horizontal plane in order to minimize effects of gravity on its performance.

Data are presented to show the comparisons of experimentally determined values of the overall heat-transfer coefficients, the condensing lengths, and the overall pressure drops with the corresponding predicted condenser characteristics. A discussion of the methods used to predict these values is also presented.

The experimental data were taken during the system performance tests described in reference 2, with a constant coolant flow rate in the shell, and two set values of coolant inlet temperature. The comparisons are presented over a range of pressure drops from 0.2 to 9.0 pounds per square inch differential, condensing lengths from 10 to 110 inches, and overall heat-transfer coefficients from 450 to 650 Btu per hour per square foot per ^{o}F.

APPARATUS

Facility

The water system (described in detail in ref. 2) was composed of three complete

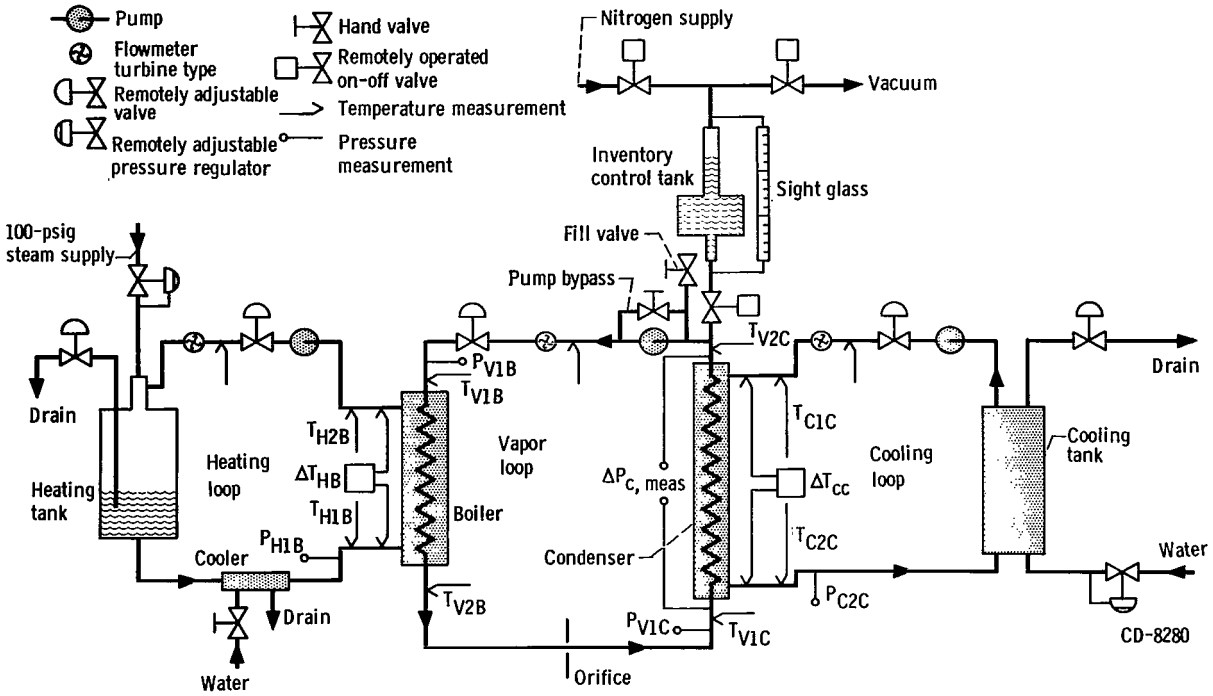

Figure 1. - Water facility schematic flow and instrumentation diagram.

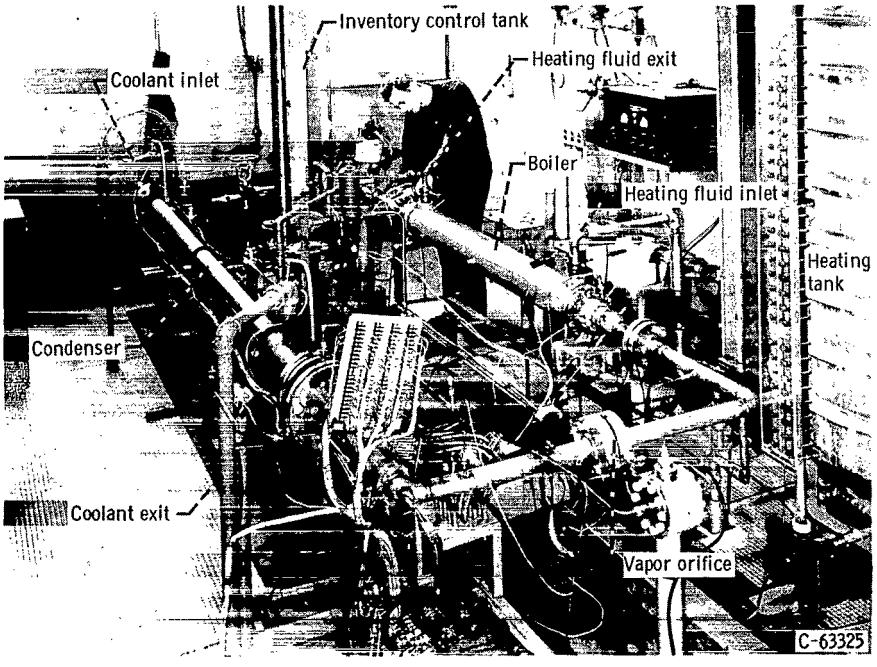

Figure 2. - Test facility.

fluid circuits: a heating loop, a cooling loop, and a vapor loop. The heating loop supplied heat to boil the water in the vapor loop, and the cooling loop removed the heat of condensation and the necessary condensate subcooling from the vapor loop. A schematic flow diagram of the three loops is presented in figure 1. The symbols used are defined in appendix A. Also included in figure 1 are the control and instrumentation locations. A photograph of the installation is shown in figure 2.

Condenser

The condenser consisted of 19 stainless-steel tubes, each approximately 10 feet long, with an outside diameter of 5/16 inch and a wall thickness of 0.035 inch. A sketch of the condenser is shown in figure 3, and a discussion of the design procedure used for this condenser is presented in appendix B. Vapor was distributed to the tubes from the inlet plenum, and the condensate was collected in the outlet plenum. The coolant in the shell was in counterflow to the vapor in the tubes, and no baffles were used to introduce cross flow. The shell was constructed with a concentric arrangement at the coolant outlet to provide uniform coolant flow as close to the vapor inlet as possible. The instrumentation channels noted in figure 3 were completely filled with thermocouples and/or wire

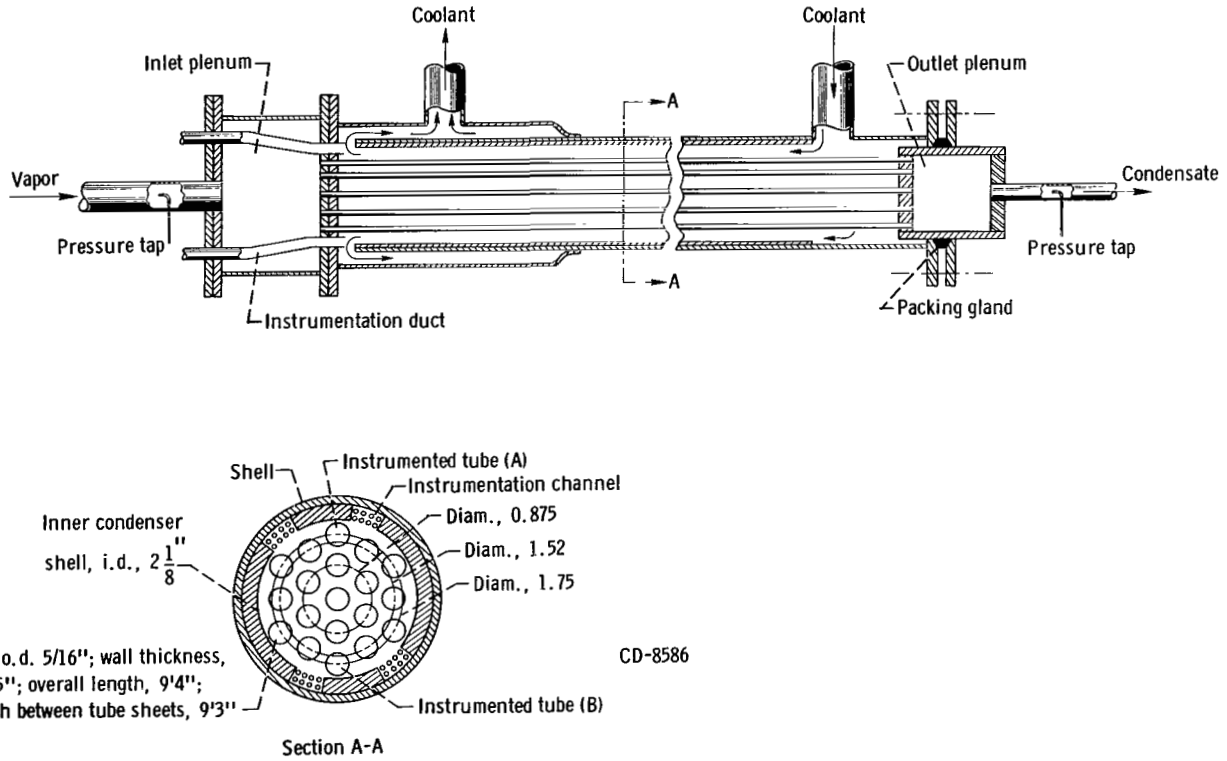

Figure 3. - Schematic diagram of 19-tube condenser.

rods and soft solder to form a smooth inside diameter for the inner condenser shell.

Instrumentation

The flow rate in each loop was measured with a turbine flowmeter placed near the pump outlet (fig. 1). Temperatures at the inlet and outlet of the boiler in the heating and vapor loops and at the inlet and outlet of the condenser in the vapor and cooling loops were measured with Chromel-Alumel thermocouples. These temperatures were read on a self-balancing potentiometer. The estimated accuracy of the reading was $\pm 2^{\circ}$ F. The temperature changes of the heating fluid from the inlet to the outlet of the boiler and of the coolant from the inlet to the outlet of the condenser were also measured directly with differential Chromel-Alumel thermocouples and a precision potentiometer. The estimated accuracy of the reading was $\pm 2^{\circ}$ F.

Axial temperatures of the condenser were also measured. Two of the condenser tubes, designated tube A at the top and tube B at the bottom (fig. 3), were instrumented with thermocouples every 8 inches over the length of the condenser, to measure the axial variation in vapor and tube wall temperature, and every 12 inches, to measure the temperature in the coolant stream. A drawing showing the method of installation is shown in figure 4, and a photograph of a typical set of these thermocouples is shown in figure 5.

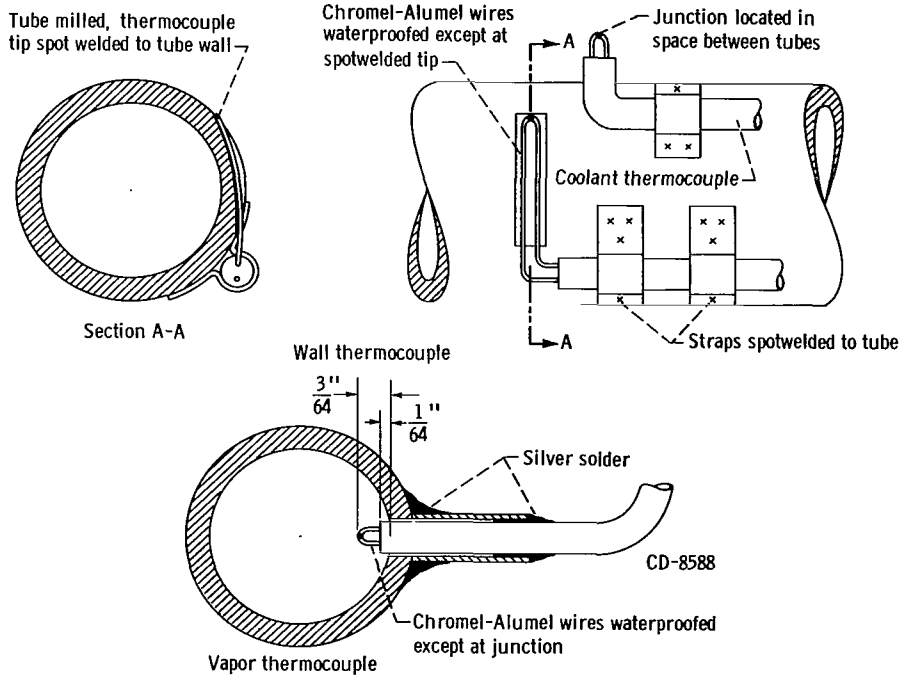

Figure 4. - Schematic diagram of condenser axial thermocouple installation.

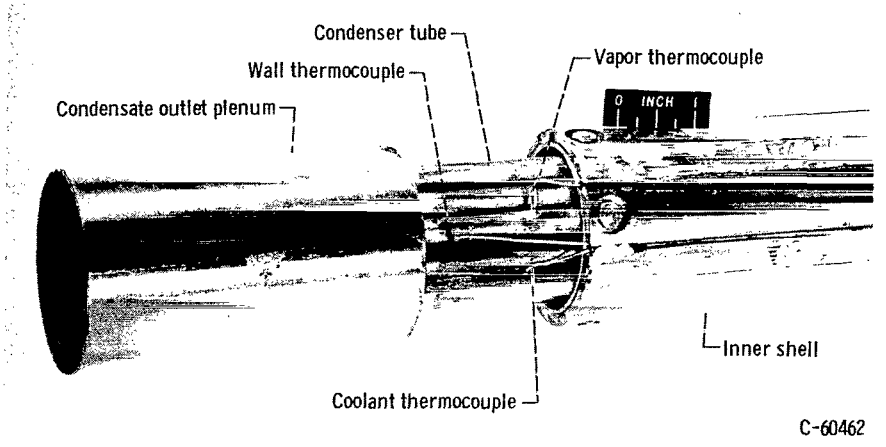

Figure 5. - Axial thermocouple installation on condenser tubes.

These thermocouples were constructed using Chromel and Alumel wires swaged with magnesium oxide insulation inside a 0.040-inch-diameter stainless-steel sheath. The temperatures were recorded on a self-balancing potentiometer. The estimated accuracy of the readings was $\pm 2^{\circ}$ F.

The total absolute pressure for the vapor loop condenser inlet was measured in the $1\frac{1}{2}$-inch pipe at the inlet plenum using a strain gage transducer rated at 15 pounds per square inch gage. Atmospheric pressure was measured with a mercury barometer. The overall vapor loop condenser pressure drop was measured directly with a differential strain gage transducer (±15 psi) connected to the inlet total pressure tap and the condensate outlet pipe. The vapor loop boiler inlet pressure was measured with a strain gage transducer rated at 0 to 25 pounds per square inch absolute. The three transducers were connected to a recording oscillograph. The estimated accuracy of the readings was ±0.35 pounds per square inch absolute for the inlet pressures and ±0.25 pound per square inch differential for the pressure drop. The pressure measuring system was calibrated at regular intervals with a mercury manometer.

EXPERIMENTAL PROCEDURE AND DATA ACQUISITION

The data in this report were obtained during the system performance tests reported in reference 2, where detailed operational procedures are also reported. As noted in reference 2, the system characteristics were such that a change in the vapor loop total inventory (i.e., total weight of fluid in the vapor loop) caused a change in the condenser inlet conditions. Therefore, some of the data were taken at constant (fixed) vapor loop

TABLE I. - RANGE OF TEST CONDITIONS

Run	Vapor loop					Cooling loop	
	Average flow rate, $\overline{W}_v$, lb/hr	Condenser inlet quality, x_o	Condenser inlet pressure, P_{V1C}, psia	Condenser inlet vapor Reynolds number, $(N_{Re})_{g,o}$	Inventory[a] (total vapor loop volume, 5.62 gal)	Average flow rate, $\overline{W}_c$, lb/hr	Condenser inlet temperature, T_{C1C}, ^oF
266 to 283	130 to 660	78 to 100	18.8 to 22.4	13 300 to 43 700	Fixed-number 1 (1.55 gal)	6090	92
285 to 298	130 to 650	67 to 100	7.8 to 18.3	13 400 to 46 200	Fixed-number 2 (1.40 gal)	6040	92
243 to 247	200	87 to 100	10.9 to 30.6	17 300 to 20 900	Variable (1.23 to 1.61 gal)	6130	120
207 to 212	235	86 to 100	12.2 to 29.4	20 300 to 25 200	Variable (1.19 to 1.62 gal)	6120	
238 to 242	280	72 to 100	15.2 to 29.9	20 300 to 30 100	Variable (1.31 to 1.67 gal)	6070	
201 to 204, 214	315	79 to 100	15.7 to 28.4	24 500 to 33 100	Variable (1.21 to 1.62 gal)	6170	
192 to 196, 213	385	54 to 100	18.4 to 30.1	21 500 to 40 300	Variable (1.21 to 1.73 gal)	6090	
233 to 237	470	69 to 88	19.8 to 23.8	33 400 to 42 200	Variable (1.27 to 1.64 gal)	6080	
197 to 200	650	40 to 61	22.9 to 27.3	26 800 to 40 900	Variable (1.44 to 1.80 gal)	5990	

[a]At room temperature.

inventory with constant coolant inlet temperature and coolant flow while the vapor loop flow was varied. The rest of the data were taken with constant vapor loop flow, coolant inlet temperature, and coolant flow, while the vapor loop inventory was varied. All data were taken after the facility had reached a steady-state condition, where the temperatures had not changed for a period of at least 15 minutes. The range of conditions covered for the experimental data is shown in table I.

DATA REDUCTION

The vapor, wall, and coolant axial temperature profiles in each of the two instrumented tubes are shown in figure 6 for a typical run. The condensing length for each tube was taken as the point at which the vapor temperature dropped abruptly (indicated by the dashed line on the figure). The measured value of condensing length $L_{c,meas}$ for the heat exchanger was considered to be the average of the two instrumented tubes A and B.

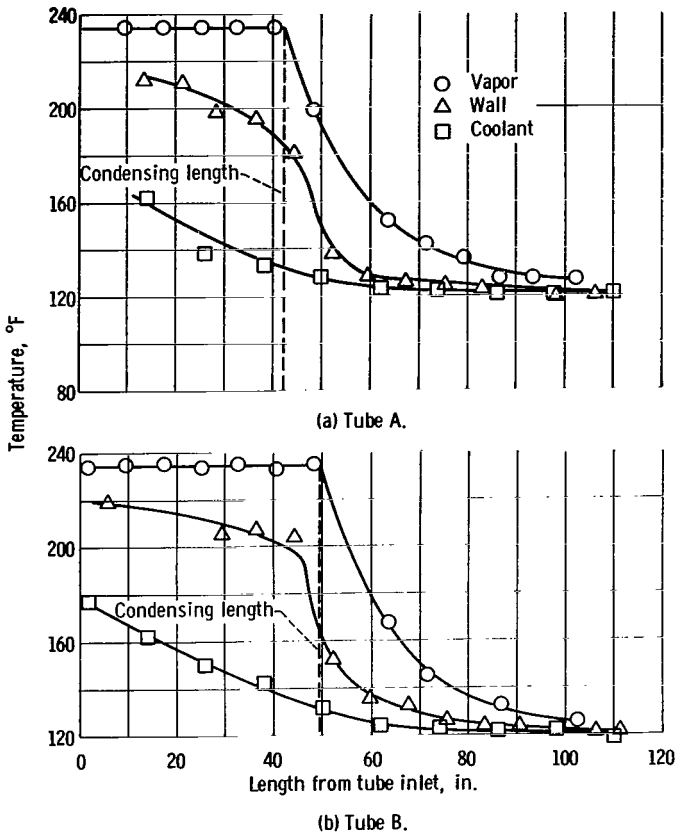

Figure 6. - Axial temperature variation in test condenser. Run 240.

The pressures and pressure drops were determined from a mean line drawn through the trace on the oscillograph record of the output of the pressure transducers. A sample oscillograph record of a typical run is shown in figure 7.

The total heat load Q_{meas}, which is the total amount of heat transferred from the heating loop to the vapor loop, or from the vapor loop to the cooling loop, was determined from the flow rate and the temperature change of the heating fluid from the inlet to the outlet of the boiler and from the flow rate and temperature change of the coolant from the inlet to the outlet of the condenser. Since these temperature changes were determined from both the direct ΔT measurement and the individually measured inlet and outlet values, four values

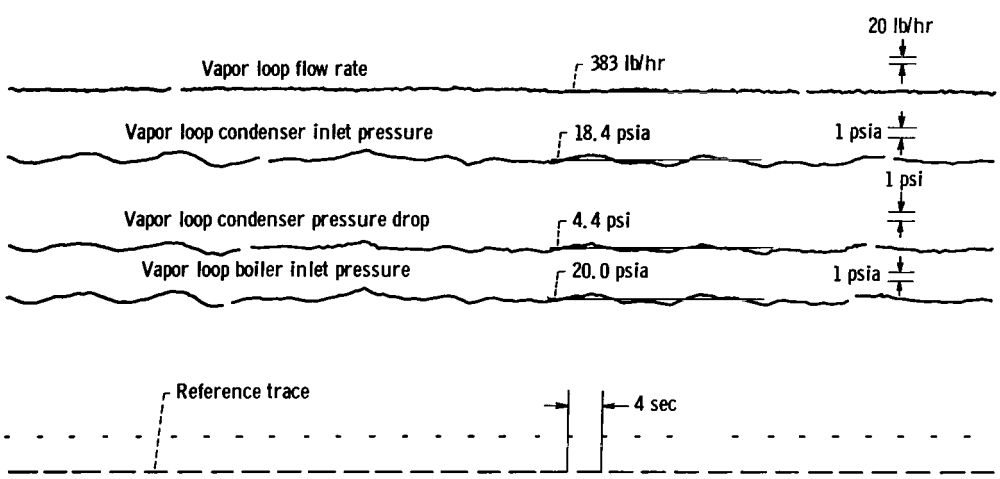

Figure 7. - Sample oscillograph record of typical steady-state operation. Run 196.

of total heat load were computed. Less than 10 percent difference existed among these values, however, and the measured value of the total heat load was taken as the average of the four calculations. The heat losses from the facility were negligible.

The vapor quality at the boiler outlet and at the condenser inlet were computed from heat balances in the boiler and condenser, respectively, using the four values of total heat load. For example, for the condenser, one value of the quality would be

$$x = \frac{W_c C_{p,\ell} \Delta T_{cc} - W_v C_{p,\ell} \left(T_{SAT,1} - T_{V2C}\right)}{W_v (h_{fg})} \tag{1}$$

Again, the difference among the values was small (< 10 percent), and the average of the four calculations was taken as the experimental value for the vapor quality at the condenser inlet x_o.

The condensing heat load then was

$$Q_c = x_o W_v (h_{fg}) \tag{2}$$

and the subcooling heat load was

$$Q_{sc} = Q_{meas} - Q_c \tag{3}$$

The experimental value of the overall heat-transfer coefficient $U_{i,c,meas}$ (over the condensing portion of the heat exchanger) was computed from the following equation:

$$U_{i,c,meas} = \frac{Q_c}{A_{hi,c} \Delta T_{LM,c}} \tag{4}$$

where

$$A_{hi,c} = N \pi D_i L_{c,meas} \tag{5}$$

and

$$\Delta T_{LM,c} = \frac{\left(T_{SAT,2} - T_{CI}\right) - \left(T_{SAT,1} - T_{C2C}\right)}{\ln\left(\frac{T_{SAT,2} - T_{CI}}{T_{SAT,1} - T_{C2C}}\right)} \tag{6}$$

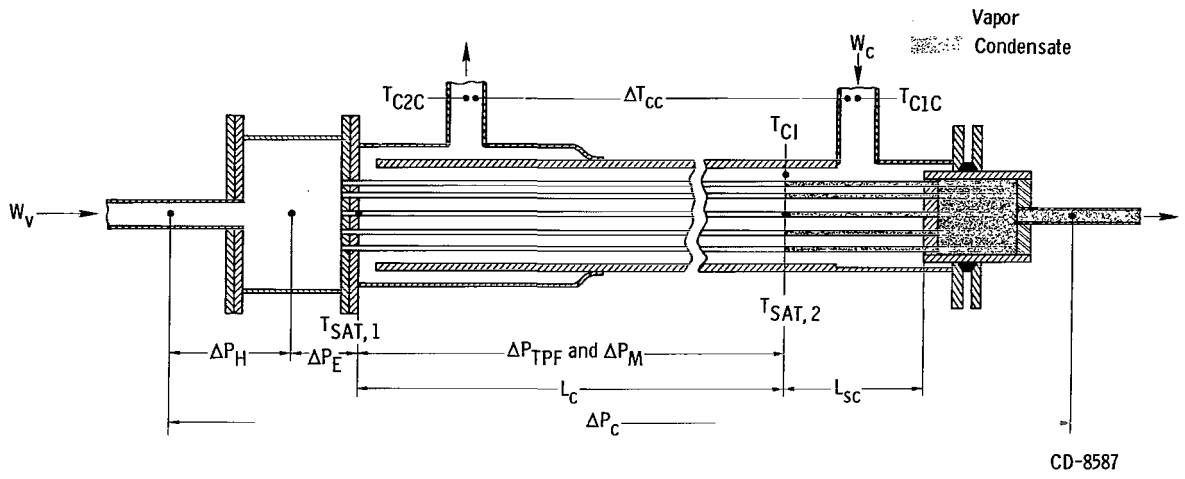

Figure 8. - Schematic diagram of test condenser showing condenser symbol usage.

The temperature of the coolant at the end of the condensing portion of the tube T_{CI} was calculated from a heat balance in the subcooling section of the heat exchanger. Values of $T_{SAT,1}$ and $T_{SAT,2}$ were taken from the vapor temperature profiles, while T_{C2C} was measured directly. A drawing showing the location of these temperatures and identifying the pressure drops and condenser lengths is presented in figure 8.

ANALYTICAL METHODS

In order to evaluate the design and performance of the condenser, predicted values of overall heat-transfer coefficient $U_{i,c,calc}$, condensing length $L_{c,calc}$, and overall pressure drop $\Delta P_{c,calc}$ were computed for each data run. Actual measured condenser inlet conditions were used in the calculations. The correlations used to calculate these predicted values and the assumptions made in order to perform the computation are presented in the following paragraphs.

Overall Heat-Transfer Coefficient

The predicted value of the overall heat-transfer coefficient (over the condensing portion of the heat exchanger) $U_{i,c,calc}$ based on the tube inside area was calculated as the reciprocal of the sum of the resistances to heat flow:

$$U_{i,c,calc} = \frac{1}{\frac{1}{h_{i,c,calc}} + \frac{t}{k_w\left(\frac{S_m}{S_i}\right)} + \frac{1}{h_{o,calc}\left(\frac{S_o}{S_i}\right)}} \tag{7}$$

It should be noted that no fouling factor was used in the calculation of $U_{i,c,calc}$.

The condensing coefficient $h_{i,c,calc}$ was obtained from the Carpenter and Colburn relation for condensation of high-velocity vapors in vertical tubes (ref. 3):

$$h_{i,c,calc} = 0.065\left(\frac{C_{p\ell}\rho_\ell k_\ell f}{2\mu_\ell \rho_g}\right)^{1/2} G_m \tag{8}$$

where

$$G_m = \sqrt{\frac{G_o^2 + G_o G_f + G_f^2}{3}} \tag{9}$$

For complete condensation, G_f becomes zero, and

$$G_m = 0.58\, G_o = \frac{0.58\, x_o W_v}{A_i} \tag{10}$$

The friction factor f was calculated for the vapor in turbulent flow, neglecting the presence of any liquid in the tube, as recommended in reference 3:

$$f = \frac{0.046}{N_{Re,g,t}^{0.2}} \tag{11}$$

where

$$N_{Re,g,t} = \frac{D_i G_m}{\mu_g} \tag{12}$$

All fluid physical properties were evaluated at the inlet saturation temperature of the vapor, $T_{SAT,1}$.

The Carpenter and Colburn relation was used for the condensing coefficient in preference to other equations because it takes into consideration the effect of vapor velocity. This correlation was derived for steam and several hydrocarbons condensing vertically downward, over a range of values for the stress at the tube wall due to vapor friction from 3.6×10^6 to 300×10^6 (lb mass/sq ft)(ft/hr^2). The range of this value in the condenser tubes was about 20×10^6 to 150×10^6 (lb mass/sq ft)(ft/hr^2).

The film coefficient $h_{o,\,calc}$ on the outside of the tubes (shell side) was calculated from the Dittus-Boelter correlation, as taken from reference 4:

$$h_{o,\,calc} = 0.023\,\frac{k}{D_E}\left(\frac{D_E G_c}{\mu}\right)^{0.8}\left(\frac{C_p\mu}{k}\right)^{0.4} \tag{13}$$

where

$$G_c = \frac{W_c}{A_s} \tag{14}$$

and

$$D_E = \frac{4A_s}{P_w} = \frac{D_s^2 - ND_o^2}{D_s + ND_o} \tag{15}$$

The Dittus-Boelter correlation was derived from data with a range of Prandtl numbers from 0.7 to 120, Reynolds numbers from 10 000 to 120 000 and a length-to-diameter ratio greater than 60. The experimental data were taken over approximate ranges of Prandtl numbers from 1 to 8, Reynolds numbers from 7 000 to 17 000, and a length-to-diameter ratio of 350. Although this relation was derived for flow inside tubes, it was considered applicable herein since the coolant flow was parallel to the tubes and only required the substitution of the equivalent diameter D_E for the inside diameter. Equation (15) was taken from reference 4 where it was used to calculate the equivalent diameter for use with flow in concentric spaces. The fluid properties for equation (13) were evaluated at an approximated average temperature of the coolant.

Condensing Length

The calculated length of the condensing portion of the counterflow heat exchanger is

defined by

$$L_{c,\,calc} = \left[\frac{Q}{N\pi D_i (U_i)\Delta T_{LM}}\right]_{c,\,calc} \tag{16}$$

The calculated length of the subcooling portion of the heat exchanger is defined by

$$L_{sc,\,calc} = \left[\frac{Q}{N\pi D_i (U_i)\Delta T_{LM}}\right]_{sc,\,calc} \tag{17}$$

The overall heat-transfer coefficient for the subcooler $U_{i,\,sc,\,calc}$ was calculated in the same manner as for the condenser (eq. 7), except that the condensing coefficient $h_{i,\,c,\,calc}$ was replaced with a subcooler tube side coefficient $h_{i,\,sc,\,calc}$ calculated using the Eubank and Proctor relation recommended in reference 4 for streamline flow in horizontal tubes:

$$h_{i,\,sc,\,calc} = 1.75\left[\frac{k_b}{D_i}\frac{W_v C_{p,\,b}}{k_b L_{sc,\,calc}} + 0.04\left(\frac{D_i}{L_{sc,\,calc}} N_{Gr} N_{Pr}\right)_b^{0.75}\right]^{1/3}\left(\frac{\mu_b}{\mu_{\ell,\,w}}\right)^{0.14} \tag{18}$$

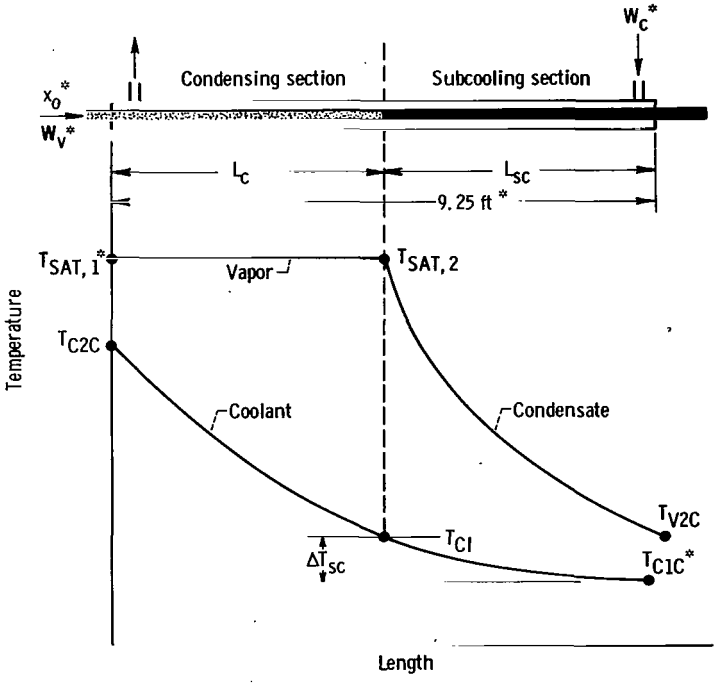

Figure 9. - Counterflow temperature profile and definition of symbols. Values marked with an asterisk were assumed known for performance predictions.

Equations (16) and (17) are related by the dimensional equation

$$\left(L_c + L_{sc}\right)_{calc} = 9.25 \text{ ft} \tag{19}$$

which gives the total length of tubes.

In order to obtain the value of the condensing length $L_{c,\,calc}$ from the dimensions of the test unit with the assumption that only the inlet flow rate and temperature conditions are known, the performance of both the condensing and subcooling portions must be evaluated. This necessity is illustrated in figure 9 for a counterflow unit. The known conditions are indicated by an asterisk.

As an approximation, $T_{SAT,2}$ was assumed equal to $T_{SAT,1}$, which assumed a negligible pressure drop. The temperature of the coolant T_{CI} at the interface location (or point in the exchanger where condensation ends and subcooling begins) is unknown. By its influence on the ΔT_{LM} of the condensing section (eqs. (6) and (16)), T_{CI} affects the length required to condense the vapor $L_{c,calc}$; however, the value of T_{CI} depends upon the amount of subcooling possible (Q_{sc} in eq. (17)) and the value of the length available after condensation $L_{sc,calc}$. Therefore, the value of T_{CI} must be obtained by simultaneously satisfying the thermal performances of both the condensing and subcooling sections of the test unit.

By writing heat balances around the condensing and subcooling sections and by properly substituting these values into the foregoing equations ((7) to (19)), a system of two equations with two unknowns (L_c and $T_{C2C})_{calc}$ was then derived. The equations were solved by trial and error using a digital computer.

Overall Pressure Drop

The overall condenser pressure drop $\Delta P_{c,calc}$ was calculated as the sum of the several pressure changes from the inlet total pressure measuring station to the outlet measuring station of the heat exchanger (figs. 3 and 8). For the condenser configuration of figure 8, it can be seen that the overall pressure change is composed of (1) the pressure loss from the inlet piping to the inlet (vapor) plenum ΔP_H, (2) the pressure change at the tube inlet ΔP_E, (3) the two-phase friction pressure loss ΔP_{TPF} over the condensing length of the tube, and (4) the momentum pressure recovery ΔP_M in the tube. The pressure drop of the liquid in the subcooling portion of the tubes, the outlet plenum, and the outlet pipe was considered negligible because of the low velocity (< 1 ft/sec). Since the heat exchanger was horizontal, there was no pressure change due to a difference in elevation from inlet to outlet. The flow area of the vapor plenum was considered large enough (20 times the total tube flow area) for the vapor velocity to be very low and the plenum to be treated as a reservoir. Therefore,

$$\Delta P_{c,calc} = \Delta P_H + \Delta P_E + \Delta P_{TPF} - \Delta P_M \tag{20}$$

The pressure loss from the inlet piping to the inlet (vapor) plenum was assumed equal to 100 percent of the velocity head in the piping. Thus,

$$\Delta P_H = \frac{\rho_g V_{g,p}^2}{2g_c} \tag{21}$$

The vapor density was based on the measured total pressure in the pipe. Since the velocity head in the piping was very small, the static pressure was very nearly equal to the total pressure in the pipe, and the error in vapor density was considered negligible.

The pressure change at the tube inlet was taken as one velocity head plus an assumed loss of 10 percent of the velocity head in the tube at the inlet due to the entrance configuration. Selection of the nominal loss of 10 percent was based on the single-phase pressure loss values of reference 5. The flow was considered virtually incompressible since the velocity head was normally less than 5 percent (6.7 percent maximum) of the static pressure at the tube inlet. Thus,

$$\Delta P_E = \frac{1.1 \rho_g V_{g,o}^2}{2 g_c} \tag{22}$$

The vapor density was based on the calculated static pressure in the inlet plenum. (Since the velocity of the vapor in the plenum was negligible, the static pressure was considered equal to the total pressure.)

Several methods have been proposed for the calculation of the friction pressure drop with two-phase flow inside horizontal tubes. The most widely used of these methods are based on the Lockhart-Martinelli correlation for isothermal two-phase, two-component flow (ref. 6). Use of this correlation to calculate the friction pressure drop during condensing requires a time-consuming, step-by-step solution. An approximating equation based on reference 6 was presented by Coombs, Stone, and Kapus (ref. 7) for the viscous liquid-turbulent gas flow regime. Their equation assumed a vapor quality of 100 percent at the condenser tube inlet. In appendix C of the present report, approximating equations for both the viscous-liquid - turbulent-gas and the turbulent-liquid - turbulent-gas regimes, which include the inlet quality as a variable, are derived for the friction pressure drop of two-phase condensing flow in a manner similar to that of reference 7.

The two-phase friction pressure loss over the condensing length of the tube was calculated by using the derived approximating equations as follows: For the viscous-liquid - turbulent-gas regime,

$$\left(\Delta P_{TPF}\right)_{VT} = \frac{\alpha_V \beta_V W_v^{1.7}}{N^{1.7} D_i^{4.7}} L_c \tag{23}$$

which for the condenser used in this report is evaluated as

$$\left(\Delta P_{TPF}\right)_{VT} = 6.14\times10^{5}\,\alpha_V\beta_V W_v^{1.7}\,L_c \tag{24}$$

For the turbulent-liquid - turbulent-gas regime,

$$\left(\Delta P_{TPF}\right)_{TT} = \frac{\alpha_T\beta_T W_v^{1.8}}{N^{1.8}D_i^{4.8}}\,L_c \tag{25}$$

which for the condenser used in this report is evaluated as

$$\left(\Delta P_{TPF}\right)_{TT} = 6.78\times10^{5}\,\alpha_T\beta_T W_v^{1.8}\,L_c \tag{26}$$

The fluid properties were based on the calculated tube inlet static pressure. It should be noted that both the measured and calculated values of condensing length $L_{c,\,meas}$ and $L_{c,\,calc}$ were used for the calculation of ΔP_{TPF}. This yielded two values for ΔP_{TPF} and two values for the calculated overall pressure drop $\Delta P_{c,\,calc}$.

The momentum pressure recovery was calculated from the standard relation

$$\Delta P_M = \frac{\rho_g V_{g,o}^2}{g_c} \tag{27}$$

The vapor density was based on the calculated tube inlet static pressure.

RESULTS AND DISCUSSION

The experimental data consisting of the flow rates, the inlet and outlet temperatures and pressures in the heating, vapor, and coolant loops measured at the locations shown in figure 1 (p. 3) are tabulated in table II. Also shown in table II are the experimental values determined for the condensing length $L_{c,\,meas}$, the heat load Q_{meas}, the vapor quality x_o, and the overall heat-transfer coefficient $U_{i,\,c,\,meas}$, as well as the predicted values of $U_{i,\,c,\,calc}$, $L_{c,\,calc}$, and $\Delta P_{c,\,calc}$.

The experimental data from the axial temperature profile thermocouples on the two instrumented tubes (tubes A and B) are tabulated in table III for the vapor temperatures

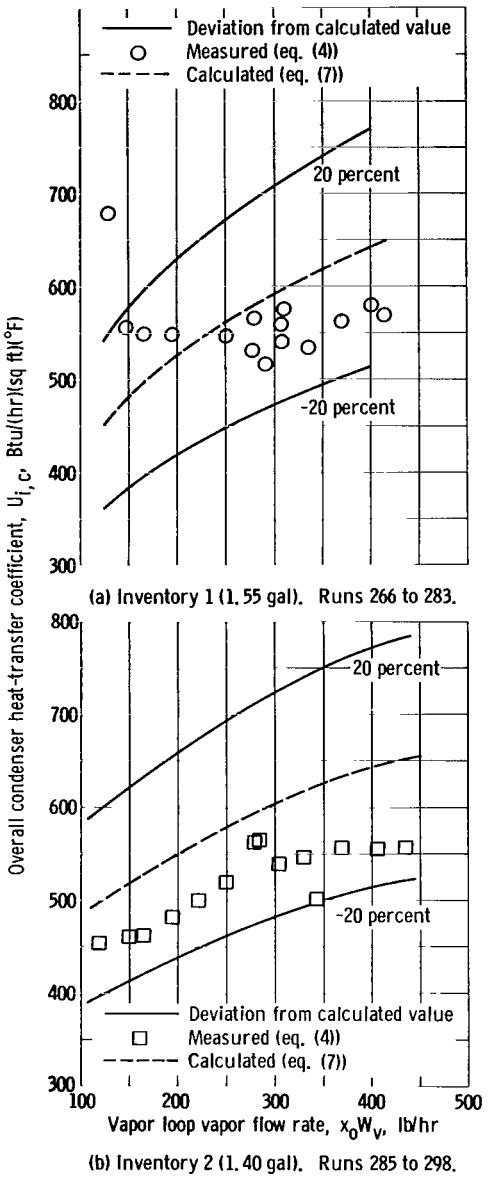

Figure 10. - Comparison of measured and calculated overall heat-transfer coefficients for fixed inventory experiments.

for all runs, and in tables IV and V for the wall and coolant temperatures for several typical runs. The axial locations of these thermocouples are also noted in the tables.

The comparisons of the measured and calculated values of overall heat-transfer coefficient $U_{i,c,meas}$ and $U_{i,c,calc}$; condensing length $L_{c,meas}$ and $L_{c,calc}$; and overall pressure drop $\Delta P_{c,meas}$ and $\Delta P_{c,calc}$ are presented in the following paragraphs. The comparisons were made graphically with the measured data plotted against the respective predicted values. In addition, with the data from the two fixed inventory experiments (designated inventories 1 and 2 in table I), both the measured and calculated values were plotted against the vapor loop vapor flow rate. It should be noted that the vapor loop condenser inlet conditions were not constant with a fixed inventory. Changes in the inlet vapor pressure, temperature, and quality occurred with changes in the vapor loop flow rate (ref. 2).

Overall Heat-Transfer Coefficient

The predicted values of the overall heat-transfer coefficient for the condenser $U_{i,c,calc}$ were calculated from equation (7), and the measured values $U_{i,c,meas}$ were determined by using equation (4). The calculations showed that the shell-side film coefficient $h_{o,calc}$ was the controlling factor in the transfer of heat. This can also be seen from the experimental data of figure 6 (p. 8), where the temperature difference between the wall and the coolant is larger than that between the vapor and the wall in the condensing portion of the tube.

The comparison of $U_{i,c,calc}$ with $U_{i,c,meas}$ for the two fixed inventories (inventories 1 and 2) is shown in figures 10(a) and (b). The figure shows that

TABLE II. - EXPERIMENTAL

Run	Heating loop				Cooling loop				Vapor					
	Boiler inlet temperature, T_{H1B}, °F	Boiler outlet temperature, T_{H2B}, °F	Boiler temperature drop, ΔT_{HB}	Flow rate, W_H, lb/hr	Condenser inlet temperature, T_{C1C}, °F	Condenser outlet temperature, T_{C2C}, °F	Coolant temperature rise, ΔT_{cc}, °F	Flow rate, W_c, lb/hr	Boiler inlet temperature, T_{V1B}, °F	Boiler outlet temperature, T_{V2B}, °F	Condenser inlet temperature, T_{V1C}, °F	Condenser outlet temperature, T_{V2C}, °F	Flow rate, W_v, lb/hr	Boiler inlet pressure, P_{V1B}, psia
192	300	256	----	8099	122	185	66.2	6037	164	230	228	166	381	21.6
193	↓	263	----	8069	122	175	54.8	6136	136	241	240	134	385	26.3
194		272	30.4	8057	121	162	43.1	6038	132	250	250	130	393	30.9
195		258	43.8	8087	121	180	61.7	6038	142	235	233	140	385	23.5
196		254	47.4	8104	120	181	64.4	6188	184	226	222	188	383	20.0
197		256	46.1	8097	122	183	65.2	5987	152	238	236	152	677	25.6
198		263	39.2	8047	122	174	55.8	5988	143	245	244	142	660	27.6
199		253	49.3	8106	120	186	69.5	5989	174	237	233	176	634	24.6
200	↓	252	49.7	8110	120	186	69.9	5989	194	236	233	196	653	24.7
201	301	263	39.6	8094	119	172	55.6	6140	155	218	214	152	309	16.8
202	300	262	39.6	8098	120	175	58.3	5892	141	226	224	138	314	19.9
203	302	265	38.0	8061	122	174	52.9	6184	135	234	234	132	321	24.2
204	302	271	32.2	8036		165	45.6	6184	132	246	246	128	309	29.3
207	300	273	28.9	8055		160	40.8	6285	126	230	230	124	230	22.5
208	↓	272	30.1	8059		164	43.4	6135	130	252	252	126	230	16.0
209		270	30.3	8040	↓	166	45.0	6035	137	262	262	134	243	13.4
210		272	27.9	8059	120	162	43.6	5989	128	236	236	122	241	24.9
211		272	28.3	8030	119	158	41.0	6140	127	242	242	121	235	27.7
212		275	26.4	8045	124	160	38.7	6034	129	249	249	126	235	30.9
213		262	39.5	8073	122	175	56.0	6136	134	240	240	130	390	----
214	↓	262	40.1	8120	123	176	56.8	6035	139	221	221	138	315	18.7
233	301	259	42.8	8155	121	179	59.8	6137	137	239	237	137	473	24.4
234	300	256	45.4	8167	122	184	63.2	6037	148	235	232	146	468	22.6
235	↓	254	47.6	8175	122	188	67.4	6135	165	231	229	167	473	21.4
236		254	48.4	8085	121	187	68.1	6038	188	230	226	190	450	20.7
237		253	49.3	8108	122	188	69.1	6037	196	230	227	202	477	21.3
238	↓	266	36.2	8084	122	171	50.4	6037	136	217	214	132	286	16.1
239	301	267	34.4	8078	123	172	50.2	6035	132	226	224	128	276	19.1
240	300	268	34.2	8123	121	168	----	6038	129	236	234	125	279	22.9
241	301	270	29.5	8110	122	165	----	6036	128	244	244	125	286	26.9
242	300	273	28.0	8079	122	158	----	6186	130	249	249	125	282	29.7
243	↓	278	22.8	8011	121	152	----	6137	128	251	251	122	198	30.2
244		276	25.2	8015	121	155	36.0	6136	129	235	235	123	198	22.6
245		277	25.2	7992	121	157	27.6	6185	128	254	255	123	193	17.1
246	↓	276	25.2	8020	124	158	----	6182	130	257	264	125	202	13.5
247	301	277	25.2	8039	122	159	----	6035	131	242	259	126	198	11.1

[a]At room temperature.

AND CALCULATED DATA

loop				Heat load, Q_{meas}, Btu/hr	Vapor quality, x_o	Differential condenser pressure drop, $\Delta P_{c, calc}$, psi	Overall heat-transfer coefficient, $U_{i, c, meas}$, Btu/(hr)(sq ft)(^oF)	Overall heat-transfer coefficient, $U_{i, c, calc}$, Btu/(hr)(sq ft)(^oF)	Condensing length, $L_{c, calc}$, in.
Condenser inlet pressure, P_{V1C}, psia	Condenser pressure loss, $\Delta P_{c, meas}$, psia	Inventory,[a] gal (total vapor loop volume, 5.62 gal)	Condensing length, $L_{c, meas}$, in.						
20.1	3.49	1.35	104.0	38.46×10^4	0.985	3.73	551	673	78.5
25.1	.93	1.62	52.5	32.30	.771	1.08	626	632	51.5
30.1	.21	1.73	25.0	24.85	.544	.25	772	563	34.3
22.1	1.77	1.51	67.5	35.75	.875	1.87	643	651	64.3
18.4	4.40	1.21	110.0	38.49	1	4.42	582	682	82.7
24.0	3.00	1.66	64.5	37.47	.498	2.97	664	647	62.7
27.3	1.00	1.80	40.0	31.78	.400	1.20	709	604	45.8
22.9	5.48	1.50	91.5	40.30	.600	5.11	598	667	74.1
22.9	6.27	1.44	93.5	40.56	.606	5.59	604	671	78.0
15.7	2.64	1.21	96.0	32.63	1	3.03	528	654	73.5
19.0	1.65	1.34	79.0	32.87	.999	2.12	551	637	65.4
23.2	.93	1.47	62.5	31.49	.922	1.29	544	638	53.3
28.4	.29	1.62	39.2	26.59	.786	.49	588	594	39.0
21.1	----	1.51	44.2	23.92	.976	.57	552	597	41.1
14.8	----	1.34	64.0	25.02	1	1.22	540	615	53.7
12.2	----	1.19	85.5	25.64	.953	2.09	528	623	64.3
23.6	----	1.53	38.5	23.49	.906	.44	571	575	38.7
26.3	----	1.59	30.5	23.76	.943	.30	670	575	36.0
29.4	----	1.62	26.2	21.89	.859	.21	699	556	33.0
----	----	1.63	48.5	32.71	.769	----		---	----
17.3	----	1.33	81.5	32.75	.994	2.37	603	651	70.6
23.8	1.70	1.64	57.7	35.77	.686	2.06	683	648	58.0
22.0	3.03	1.53	77.5	37.58	.750	3.23	617	660	68.4
20.6	4.36	1.41	99.0	39.88	.811	4.87	629	683	79.5
19.8	5.21	1.32	110.0	39.78	.878	5.47	605	681	83.7
20.3	5.64	1.27	105.0	40.40	.847	5.53	640	683	86.2
15.5	1.60	1.31	77.0	29.57	.986	2.06	592	639	66.2
18.8	.80	1.41	57.2	29.17	1	1.19	641	629	57.0
22.7	.48	1.51	46.0	27.69	.925	.74	626	608	46.6
26.7	.32	1.61	34.2	26.07	.835	.42	686	587	39.6
29.9	.16	1.67	23.5	22.47	.715	.19	759	558	32.0
30.6	.00	1.61	18.7	18.76	.872	.10	769	527	27.4
22.7	.11	1.53	31.2	20.38	.987	.28	609	563	34.1
17.0	.32	1.42	42.5	21.23	1	.50	577	580	41.0
13.4	.58	1.31	51.2	20.57	.913	.75	557	589	47.1
10.9	.96	1.23	73.7	20.91	.965	1.39	487	597	56.1

TABLE II. - Concluded. EXPERIMENTAL

Run	Heating loop				Cooling loop				Vapor					
	Boiler inlet temperature, T_{H1B}, °F	Boiler outlet temperature, T_{H2B}, °F	Boiler temperature drop, ΔT_{HB}	Flow rate, W_H, lb/hr	Condenser inlet temperature, T_{C1C}, °F	Condenser outlet temperature, T_{C2C}, °F	Coolant temperature rise, ΔT_{cc}, °F	Flow rate, W_c, lb/hr	Boiler inlet temperature, T_{V1B}, °F	Boiler outlet temperature, T_{V2B}, °F	Condenser inlet temperature, T_{V1C}, °F	Condenser outlet temperature, T_{V2C}, °F	Flow rate, W_v, lb/hr	Boiler inlet pressure, P_{V1B}, psia
266	301	266	37.6	8059	93	142	51.5	6074	104	235	234	99	278	23.3
267	↓	266	36.6	8107	92	140	51.8	6176	104	233	234	98	278	23.3
268		269	33.4	8046	92	136	47.2	6175	103	236	236	96	252	22.9
270		276	26.3	8020	92	128	37.3	6074	102	236	235	94	204	23.9
271		280	22.0	8003	92	122	32.2	6075	102	237	236	93	174	23.8
272		282	19.5	8041	91	119	29.9	6076	102	237	236	92	156	23.4
273	↓	286	16.4	8001	90	113	24.2	6028	104	235	235	91	129	23.2
274	300	263	39.2	8163	90	142	54.2	6077	104	236	235	98	303	23.1
275	301	262	41.4	8145	92	147	58.4	6075	108	235	235	104	330	23.0
276	301	258	45.0	8112	92	152	62.8	6075	113	236	234	108	392	22.9
277	302	254	49.3	8104	92	158	69.7	6075	122	234	230	120	472	22.2
278	300	247	54.2	8081	92	163	75.0	6075	144	230	227	144	664	21.3
280	300	247	55.1	8179	91	163	76.4	6176	147	231	227	146	656	21.5
282	300	260	41.4	8102	92	147	57.7	6075	110	235	234	104	352	22.8
283	300	260	41.5	8128	92	147	58.2	6075	110	235	234	105	357	23.0
285	300	264	37.0	8065	92	143	53.7	6026	104	216	216	100	284	16.2
286	↓	264	37.0	8114	92	143	53.7	6025	105	217	216	100	280	16.5
287		267	33.8	8052	91	136	48.9	6027	102	215	212	96	252	15.4
288		270	29.9	8040	92	134	44.0	6025	102	254	254	96	229	15.1
289		274	26.8	8024	93	130	38.7	6074	103	262	262	96	204	14.5
290		278	22.9	8007	92	124	34.0	6025	103	256	259	94	174	12.6
291		281	20.0	8020	92	121	29.4	6024	104	262	253	93	154	11.1
292		285	16.0	8028	92	115	25.0	6026	106	255	249	92	129	8.8
293		262	39.7	8124	93	148	56.9	6074	109	221	219	104	303	17.5
294	↓	258	43.9	8089	93	152	61.5	6074	112	224	222	108	330	18.7
295	301	254	48.0	8103	92	157	68.3	6025	122	225	224	119	385	19.4
296	301	250	52.0	8142	91	162	74.1	6026	136	224	224	134	451	19.7
297	300	246	54.8	8179	93	166	77.3	6074	179	230	227	180	651	21.3
298	300	257	44.1	8140	92	152	64.2	6075	115	225	221	110	356	19.1

[a]At room temperature.
[b]Fixed inventory 1.
[c]Fixed inventory 2.

AND CALCULATED DATA

loop				Heat load, Q_{meas}, Btu/hr	Vapor quality, x_o	Overall condenser pressure drop, $\Delta P_{c, calc}$, psi	Overall heat-transfer coefficient, $U_{i, c, meas}$, Btu/(hr)(sq ft)(^oF)	Overall heat-transfer coefficient, $U_{i, c, calc}$, Btu/(hr)(sq ft)(^oF)	Condensing length, $L_{c, calc}$, in.
Condenser inlet pressure, P_{V1C}, psia	Condenser pressure loss, $\Delta P_{c, meas}$, psia	Inventory,[a] gal (total vapor loop volume, 5.62 gal)	Condensing length, $L_{c, meas}$, in.						
21.2	0.48	1.56	44.2	30.09×10^4	0.995	0.80	531	580	41.8
21.4	.58	1.55	42.2	30.20	1	.75	565	582	41.1
21.2	.42	(b)	38.0	27.41	.995	.57	546	568	37.4
22.2	.11		28.0	21.40	.959	----	548	524	29.5
22.4	.05		22.5	18.29	.957	.15	549	497	25.5
22.0	.00		19.2	16.23	.949	.10	556	479	23.2
21.7	.05		13.5	13.97	.999	.06	679	454	20.9
21.4	.74		47.7	31.98	.965	.97	516	583	43.4
21.1	1.01		47.7	33.83	.939	1.10	577	596	46.9
21.0	1.44		58.5	36.93	.858	1.67	534	610	51.7
20.0	2.77		68.0	40.62	.784	3.19	561	627	59.2
18.8	6.17		84.2	44.15	.604	6.00	579	641	68.3
18.9	6.33		88.5	45.33	.633	6.52	568	649	69.0
21.1	1.01	▼	49.2	33.82	.873	1.17	560	595	46.7
21.2	1.12	1.55	50.7	33.98	.865	1.21	541	595	46.9
14.4	.96	1.41	52.7	30.79	1	1.43	565	595	51.8
14.6	.96	1.40	53.2	30.70	1	1.40	561	593	51.8
13.6	.74	(c)	50.5	27.78	1	1.17	519	578	47.8
13.4	.48		45.7	24.98	.971	.86	499	564	41.7
13.0	.43		42.0	22.15	.955	.65	482	549	37.1
11.3	.21		37.5	18.89	.953	.50	462	528	34.2
9.8	.16		36.0	17.15	.975	.44	460	520	33.3
7.8	.16		30.2	13.79	.931	.30	455	496	30.4
15.6	1.17		61.0	32.91	1	1.76	539	606	54.0
16.7	1.54		64.0	35.82	1	2.03	546	616	57.6
16.9	2.61		74.0	39.62	.962	2.96	557	629	64.8
17.3	4.10		87.0	43.03	.900	4.23	554	640	71.0
18.3	8.62	▼	101.0	45.30	.672	8.15	556	654	77.0
17.0	1.81	1.40	71.7	36.93	.963	2.48	501	619	58.5

TABLE III. - CONDENSER AXIAL

Run	Tube A														
															Thermo-
	T_{A-1}	T_{A-2}	T_{A-3}	T_{A-4}	T_{A-5}	T_{A-6}	T_{A-7}	T_{A-8}	T_{A-9}	T_{A-10}	T_{A-11}	T_{A-12}	T_{A-13}	T_{A-14}	T_{A-15}
															Location, in.
	2.0	9.7	17.4	25.1	32.9	40.5	48.2	56.0	63.7	71.4	79.1	86.8	93.9	102.2	110.0
															Vapor
192	(a)	225	226	225	225	222	220	(a)	219	217	215	216	214	176	(a)
193		240	240	239	240	238	208		177	164	161	154	150	146	
194		238	230	214	204	195	182		166	164	157	149	149	145	
195		231	232	229	229	230	228		207	188	171	154	148	143	
196		217	218	219	216	216	213		210	210	210	208	208	208	
197		235	230	230	231	225	216		204	197	186	177	173	168	
198		240	238	229	223	217	205		192	189	182	172	170	166	
199		231	227	227	224	221	220		217	217	202	190	182	167	
200		224	227	225	223	221	220		216	217	211	197	185	167	
201		211	211	211	210	209	208		205	205	205	204	204	168	
202		222	222	222	220	224	224		220	220	197	170	150	140	
203		239	238	236	237	237	234		200	176	154	146	142	135	
204		247	248	246	221	208	185		165	158	148	145	140	139	
207		230	232	228	229	230	166		135	134	130	124	124	124	
208		211	217	212	209	210	210		208	164	142	131	129	127	
209		202	202	202	201	199	198		194	196	195	191	152	141	
210		239	239	239	237	176	150		134	132	127	124	124	124	
211		242	244	237	196	162	141		130	127	126	122	122	122	
212		244	246	197	174	162	147		139	139	136	132	131	130	
213		239	239	238	237	237	194		169	157	156	145	141	139	
214		218	217	217	217	217	217		215	214	208	163	151	140	
233		233	236	234	234	230	211		188	174	165	157	149	146	
234		229	230	230	226	228	225		220	196	178	156	153	147	
235		225	225	224	222	222	220		217	215	212	211	190	164	
236		221	222	220	219	220	218		210	213	211	210	210	210	
237		224	224	219	221	219	213		212	212	210	211	211	201	
238		211	211	210	211	210	211		209	209	188	151	142	135	
239		224	220	224	224	222	224		188	160	143	136	134	130	
240		234	234	234	234	234	199		152	142	136	128	128	127	
241		240	244	240	213	186	162		143	141	139	133	133	132	
242		240	224	202	194	181	168		155	151	146	141	140	138	
243		245	196	163	162	156	143		132	132	130	125	125	125	

[a]Thermocouple failed.

VAPOR TEMPERATURES

Tube B														
couple														
T_{B-1}	T_{B-2}	T_{B-3}	T_{B-4}	T_{B-5}	T_{B-6}	T_{B-7}	T_{B-8}	T_{B-9}	T_{B-10}	T_{B-11}	T_{B-12}	T_{B-13}	T_{B-14}	T_{B-15}
from tube inlet														
2.0	9.7	17.4	25.1	32.8	40.5	48.2	55.9	63.7	71.4	79.2	86.8	93.9	102.3	110.0
temperature, ^{o}F														
226	225	226	224	224	223	223	(a)	220	220	(a)	219	(a)	219	(a)
241	240	240	240	239	238	238	↓	238	195	↓	157	↓	138	↓
251	250	247	247	250	250	202	↓	148	137	↓	132	↓	126	↓
234	232	231	231	232	228	230	↓	228	228	↓	183	↓	155	↓
219	217	218	216	215	215	214	↓	210	210	↓	210	↓	210	↓
236	236	235	232	230	231	231	↓	229	230	↓	228	↓	175	↓
244	245	244	244	243	241	244	↓	243	192	↓	159	↓	140	↓
232	231	231	227	227	226	225	↓	222	222	↓	221	↓	219	↓
233	231	230	229	224	224	222	↓	217	219	↓	216	↓	211	↓
224	213	213	210	208	208	208	↓	206	206	↓	206	↓	170	↓
224	222	223	223	221	220	219	↓	219	219	↓	193	↓	146	↓
237	236	235	235	234	233	236	↓	233	207	↓	159	↓	140	↓
248	246	246	248	248	248	247	↓	164	145	↓	134	↓	126	↓
232	230	230	232	232	232	195	↓	145	137	↓	130	↓	125	↓
226	213	211	212	212	211	209	↓	210	165	↓	136	↓	128	↓
232	201	201	200	198	198	196	↓	195	197	↓	180	↓	144	↓
239	239	239	239	239	239	186	↓	141	135	↓	128	↓	124	↓
244	244	244	244	244	208	147	↓	132	128	↓	122	↓	120	↓
251	250	251	251	250	180	153	↓	137	132	↓	129	↓	126	↓
240	239	241	239	241	241	241	↓	192	173	↓	145	↓	133	↓
215	216	217	217	217	217	217	↓	216	214	↓	173	↓	147	↓
237	236	236	233	234	233	231	↓	232	233	↓	171	↓	146	↓
230	225	227	227	225	224	224	↓	222	224	↓	226	↓	166	↓
224	224	224	221	221	221	221	↓	217	218	↓	218	↓	218	↓
224	220	222	219	220	215	214	↓	214	211	↓	212	↓	211	↓
224	223	223	223	218	216	216	↓	209	214	↓	212	↓	209	↓
225	208	212	210	210	210	210	↓	208	209	↓	168	↓	139	↓
222	224	223	224	222	223	222	↓	192	176	↓	146	↓	132	↓
234	235	235	234	235	233	235	↓	168	145	↓	133	↓	126	↓
242	243	244	244	244	244	196	↓	154	142	↓	130	↓	126	↓
250	250	250	250	250	204	166	↓	140	132	↓	126	↓	124	↓
252	252	252	252	186	165	144	↓	129	126	↓	123	↓	122	↓

TABLE III. - Concluded. CONDENSER

Run	Tube A														
															Thermo-
	T_{A-1}	T_{A-2}	T_{A-3}	T_{A-4}	T_{A-5}	T_{A-6}	T_{A-7}	T_{A-8}	T_{A-9}	T_{A-10}	T_{A-11}	T_{A-12}	T_{A-13}	T_{A-14}	T_{A-15}
															Location, in.
	2.0	9.7	17.4	25.1	32.9	40.5	48.2	56.0	63.7	71.4	79.1	86.8	93.9	102.2	110.0
															Vapor
244	(a)	235	236	233	195	152	136	(a)	127	127	125	122	122	122	(a)
245		216	219	217	214	214	158		140	134	127	123	123	123	
246		209	213	207	207	206	206		153	142	132	130	129	127	
247		197	204	197	196	195	195		192	195	152	136	132	129	
266		233	233	233	233	230	152		119	110	107	100	100	97	
267		234	234	233	231	231	151		124	111	109	99	99	97	
268		233	233	233	233	186	129		112	105	103	97	97	95	
270		236	238	201	151	130	108		100	99	96	94	94	94	
271		231	229	149	123	113	101		95	95	93	91	91	91	
272		227	177	128	113	106	97		93	93	92	90	90	90	
273		98	94	91	91	90	89		88	88	88	88	88	88	
274		234	234	234	234	234	138		124	120	114	104	102	100	
275		232	234	230	229	225	200		151	129	119	111	109	105	
276		229	226	227	227	229	224		172	147	134	126	118	112	
277		223	221	227	228	224	220		187	174	142	138	129	123	
278		219	218	213	212	211	210		207	207	186	166	153	143	
280		221	218	215	211	209	206		204	192	179	170	159	152	
282		232	230	231	231	231	203		145	132	126	111	111	107	
283		230	230	230	231	231	224		157	143	130	112	112	108	
285		214	214	216	216	214	214		158	130	114	104	102	98	
286		215	215	213	214	214	212		150	129	118	106	104	100	
287		212	216	212	212	213	211		129	114	108	100	98	96	
288		210	211	210	210	212	176		118	108	103	97	97	96	
289		209	209	209	209	209	128		105	101	98	92	92	92	
290		204	204	204	204	163	113		98	96	94	92	92	92	
291		197	206	197	197	133	104		95	95	93	91	91	91	
292		189	199	190	150	113	97		92	92	91	90	90	90	
293		212	214	214	216	215	214		182	144	125	110	109	106	
294		221	220	221	221	221	220		214	167	147	119	119	109	
295		216	218	219	219	218	217		217	216	179	138	132	116	
296		217	218	218	216	215	214		210	212	210	175	154	137	
297		220	217	213	211	208	204		200	200	197	197	188	164	
298		219	219	218	218	217	216		217	196	156	129	123	113	

[a]Thermocouple failed.

AXIAL VAPOR TEMPERATURES

Tube B														
couple														
T_{B-1}	T_{B-2}	T_{B-3}	T_{B-4}	T_{B-5}	T_{B-6}	T_{B-7}	T_{B-8}	T_{B-9}	T_{B-10}	T_{B-11}	T_{B-12}	T_{B-13}	T_{B-14}	T_{B-15}
from tube inlet														
2.0	9.7	17.4	25.1	32.8	40.5	48.2	55.9	63.7	71.4	79.2	86.8	93.9	102.3	110.0
temperature, ^{o}F														
236	236	234	237	235	165	147	(a)	134	130	(a)	125	(a)	122	(a)
218	217	215	218	215	217	170		138	130		125		122	
226	207	207	206	206	206	206		154	140		132		126	
220	197	197	197	197	200	195		194	195		138		130	
234	234	234	234	234	234	229		137	124		110		103	
232	232	232	230	230	230	194		135	126		107		99	
234	234	234	232	233	233	168		123	115		103		98	
236	236	236	236	236	153	122		115	101		96		95	
240	240	239	239	168	130	111		98	96		93		93	
238	238	238	236	151	122	106		96	95		92		92	
236	234	236	193	130	112	100		92	92		90		90	
234	234	234	234	234	234	234		154	134		112		102	
232	232	230	233	232	232	232		171	148		119		107	
231	231	232	230	230	230	230		230	182		134		114	
229	229	227	223	221	223	223		221	220		173		137	
222	221	221	218	214	213	212		208	208		206		180	
224	221	221	214	212	213	213		208	206		205		205	
232	231	228	231	231	233	232		186	153		120		108	
233	233	233	233	234	234	234		190	164		121		106	
215	215	215	215	214	212	212		166	142		116		105	
216	215	217	217	216	213	213		165	144		116		104	
213	211	211	208	209	211	209		144	127		106		99	
211	211	211	213	213	211	202		128	113		103		98	
211	208	208	208	208	208	158		115	107		98		96	
203	215	203	203	186	186	127		104	100		94		93	
198	198	197	198	158	158	118		100	97		93		93	
191	190	190	190	125	125	105		94	94		91		91	
219	217	219	219	217	217	218		189	168		122		108	
220	220	220	220	219	219	218		218	186		136		116	
221	221	221	221	217	220	217		214	214		169		131	
222	218	219	215	215	212	213		212	212		210		157	
223	220	220	215	213	210	210		202	202		200		199	
222	221	220	219	216	215	215		218	218		145		119	

TABLE IV. - CONDENSER AXIAL WALL TEMPERATURES

Run	Tube A														
	Thermocouple														
	W_{A-1}	W_{A-2}	W_{A-3}	W_{A-4}	W_{A-5}	W_{A-6}	W_{A-7}	W_{A-8}	W_{A-9}	W_{A-10}	W_{A-11}	W_{A-12}	W_{A-13}	W_{A-14}	W_{A-15}
	Location, in. from tube inlet														
	5.8	13.6	21.3	29.0	36.7	44.4	52.1	59.8	67.6	75.3	83.0	90.7	98.4	106.1	111
	Wall temperature, ^{o}F														
192	(a)	216	210	206	209	205	205	196	192	195	186	(a)	128	124	(a)
194	↓	195	170	162	164	156	154	145	138	140	136	↓	125	122	↓
201		201	198	196	196	194	194	182	181	181	170		123	121	
212		188	142	136	136	132	130	128	128	128	127		123	123	
233		218	201	201	198	188	157	143	140	140	136		124	123	
240		212	200	198	195	180	138	128	126	124	123		120	120	
271		176	106	100	96	94	93	92	92	92	91		89	89	
274		210	191	190	184	159	108	99	96	94	92		88	88	
280		204	194	194	194	188	186	172	166	156	138		112	98	
287		194	180	180	182	162	138	100	96	94	92		90	90	
292		166	134	131	97	93	92	92	91	90	90		89	89	
297		206	194	195	195	190	187	174	172	176	167		116	104	

Run	Tube B														
	Thermocouple														
	W_{B-1}	W_{B-2}	W_{B-3}	W_{B-4}	W_{B-5}	W_{B-6}	W_{B-7}	W_{B-8}	W_{B-9}	W_{B-10}	W_{B-11}	W_{B-12}	W_{B-13}	W_{B-14}	W_{B-15}
	Location, in. from tube inlet														
	5.8	13.5	21.2	29.0	36.7	44.4	52.1	59.8	67.6	75.3	83.0	90.7	98.4	106.2	111
	Wall temperature, ^{o}F														
192	220	(a)	207	214	214	209	208	172	198	172	187	191	(a)	140	128
194	229	↓	200	219	224	164	144	128	128	124	122	122	↓	120	120
201	206		194	200	200	195	194	168	187	167	178	182		128	122
212	224		196	213	158	142	134	128	128	127	125	125		124	124
233	221		208	214	216	210	207	174	199	138	137	133		125	122
240	219		199	205	207	204	152	135	133	126	124	124		121	121
271	214		180	144	116	102	96	93	93	92	90	90		90	90
274	214		190	205	205	198	173	113	108	97	96	95		90	90
280	210		197	204	204	199	198	176	187	159	170	174		140	103
287	199		177	189	188	181	185	105	105	96	93	93		90	90
292	175		157	172	116	99	94	92	92	92	90	90		89	89
297	212		196	202	202	196	194	161	184	158	172	172		158	126

[a]Thermocouple failed.

TABLE V. - CONDENSER AXIAL COOLANT TEMPERATURES

Run	Tube A										Tube B									
	Thermocouple																			
	S_{A-1}	S_{A-2}	S_{A-3}	S_{A-4}	S_{A-5}	S_{A-6}	S_{A-7}	S_{A-8}	S_{A-9}	S_{A-10}	S_{B-1}	S_{B-2}	S_{B-3}	S_{B-4}	S_{B-5}	S_{B-6}	S_{B-7}	S_{B-8}	S_{B-9}	S_{B-10}
	Location, in. from tube inlet																			
	2.0	14.0	26.0	38.0	50.0	62.0	74.0	86.0	98.0	110.0	2.0	14.0	26.0	38.0	50.0	62.0	74.0	86.0	98.0	110.0
	Coolant temperature, ^{o}F																			
192	(a)	177	169	159	155	140	(a)	127	124	123	188	183	175	172	162	151	148	136	132	122
194	↓	147	133	126	125	122	↓	121	119	120	166	155	141	133	124	122	122	122	122	120
201		167	160	151	145	135		122	119	119	172	164	160	159	150	139	136	128	122	118
212		146	129	126	126	126		125	123	124	167	152	140	130	126	126	126	126	126	124
233		164	145	139	133	124		122	120	120	183	174	161	157	146	134	126	124	123	120
240		162	138	133	128	123		121	120	121	177	162	150	142	132	124	123	122	122	119
271		110	93	92	92	92		92	90	90	130	112	100	93	92	92	91	91	91	88
274		132	110	100	96	91		90	88	89	148	129	118	111	104	93	92	91	90	88
280		156	138	132	128	108		94	93	91	167	156	148	144	135	119	114	106	100	89
287		128	109	105	98	92		91	89	89	140	129	114	109	104	94	93	92	92	89
292		107	94	92	92	91		91	90	90	119	111	99	93	91	91	91	91	91	88
297	↓	162	144	139	134	118	↓	102	100	96	170	159	150	147	139	125	120	111	104	92

[a]Thermocouple failed.

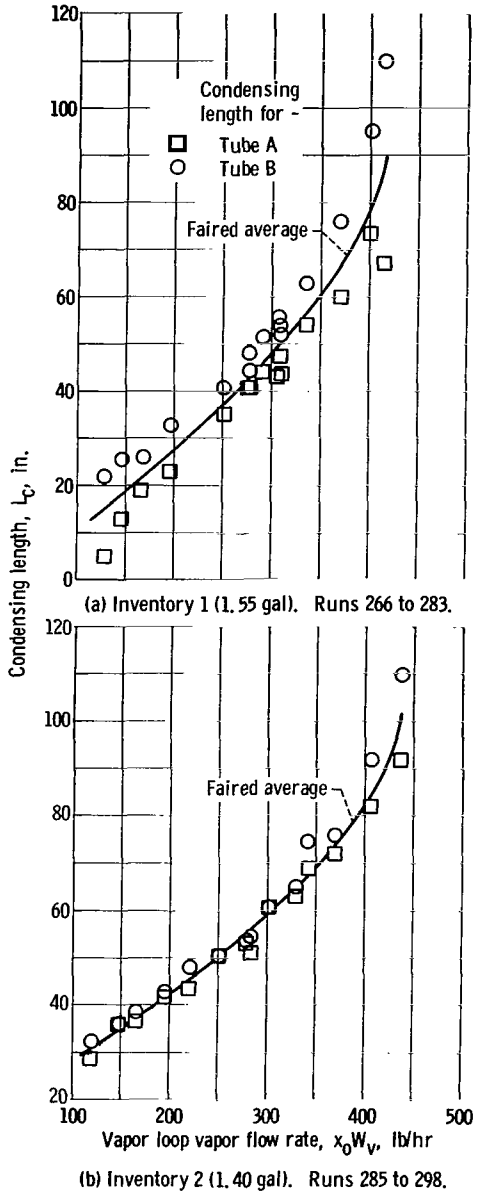

Figure 11. - Comparison of measured condensing lengths of tubes A and B with average values for fixed inventory experiments.

the predicted coefficient has a slope with respect to the flow rate. There are two reasons for the slope of the calculated curve:

(1) The shell-side coefficient $h_{o, calc}$ (eq. (13)) is affected by the temperature level of the coolant. As the vapor flow decreases, the average temperature of the coolant decreases, and $h_{o, calc}$ decreases, which causes $U_{i, c, calc}$ to decrease.

(2) Although $h_{o, calc}$ is the controlling factor, $U_{i, c, calc}$ is also affected slightly by the condensing coefficient $h_{i, c, calc}$, which also decreases with decreasing vapor flow.

The experimental data in figure 10(a) did not appear to show this trend as well as the data in figure 10(b); however, most of the experimental data are within the lines representing deviations of ±20 percent from the calculated values. Therefore, although the comparisons are not quite the same in figures 10(a) and (b), experimental data of inventories 1 and 2 show reasonable agreement with the predicted values. Nevertheless, an examination of the experimental data was made in an attempt to determine if there was any apparent reason for the slight difference in the comparisons for the two fixed inventories.

The value of $U_{i, c, meas}$ depends upon the experimental values of the heat load Q_c, the log-mean temperature difference $\Delta T_{LM, c, meas}$, and the condensing length $L_{c, meas}$ (heat-transfer area); however, it would appear that the largest percent experimental error would be in the value of $L_{c, meas}$. Therefore, the measured condensing lengths of both instrumented tubes (tubes A and B) were plotted against vapor loop vapor flow rate x_0W_v for the two fixed inventories (inventories 1 and 2), as shown in figures 11(a) and (b). As stated previously, $L_{c, meas}$ is the average value of tubes A and B, and a curve faired through the average values is shown in the figure. The differences in condensing lengths of tubes A and B are larger for inventory 1 (fig. 11(a)) than for

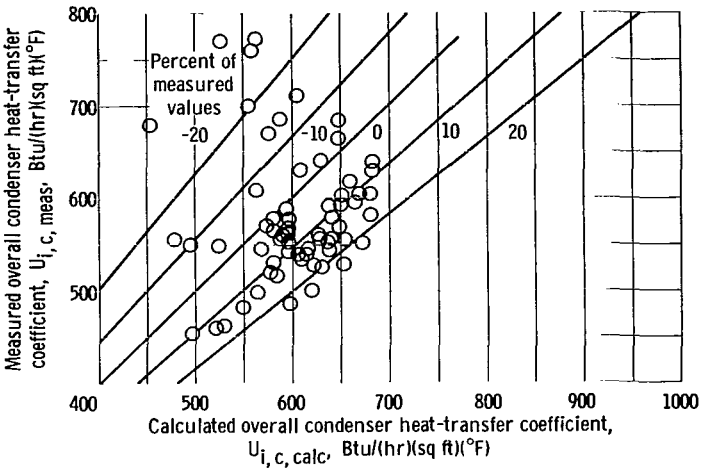

Figure 12. - Comparison of calculated and measured overall condenser heat-transfer coefficients for all runs (see table I).

inventory 2 (fig. 11(b)), and the average condensing lengths for inventory 1 at the lower flow rates are shorter than those for inventory 2.

The experimental percent error in the measured value of condensing length would increase as the condensing lengths decrease. (Since the axial thermocouples in the vapor are about 8 inches apart, the experimental accuracy is about ±4 inches.) Therefore, the condensing length data for inventory 1 would be subject to a higher percent error than the data for inventory 2, at the lower vapor flow rates. Also of significance, however, is the fact that only 2 of the 19 tubes were instrumented; therefore, if the differences in condensing length of the two tubes (tubes A and B) become large, as in figure 11(a) for inventory 1, the average values for the condensing length may become less representative of all 19 tubes. Thus, the different characteristics of the experimental condensing lengths $L_{c,meas}$ for the two fixed inventories may be one reason for the slight difference in the comparisons of the measured and calculated overall heat-transfer coefficients $U_{i,c,meas}$ and $U_{i,c,calc}$ of figure 10.

The comparison of $U_{i,c,calc}$ with $U_{i,c,meas}$ for all runs is presented in figure 12. All values of $U_{i,c,meas}$ were determined by using the average condensing length $L_{c,meas}$. Lines representing deviations of ±10 and ±20 percent from the measured values are also shown in figure 12. It can be seen that almost all the calculated values are within ±20 percent of the measured overall heat-transfer coefficient, and that the majority of the calculated values are from 0 to 20 percent higher than the measured value.

Condensing Length

The predicted values of condensing length $L_{c,calc}$ were calculated from equation (16), as stated in the section ANALYTICAL METHODS, for a vapor saturation temperature that was constant over the condensing length of the tube ($T_{SAT,2} = T_{SAT,1}$). The measured values $L_{c,meas}$ were the average condensing lengths of the two instrumented tubes (tubes A and B) as explained in the preceding paragraphs. The comparison of $L_{c,calc}$ with $L_{c,meas}$ for the two fixed inventories (inventories 1 and 2) over the range of vapor flow rates is presented in figures 13(a) and (b). The predicted values for inven-

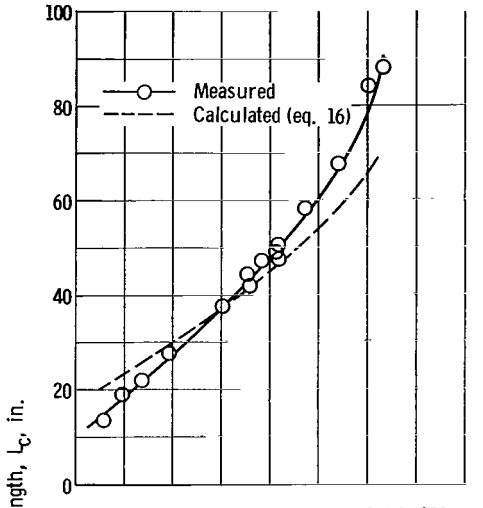

(a) Inventory 1 (1.55 gal). Runs 266 to 283.

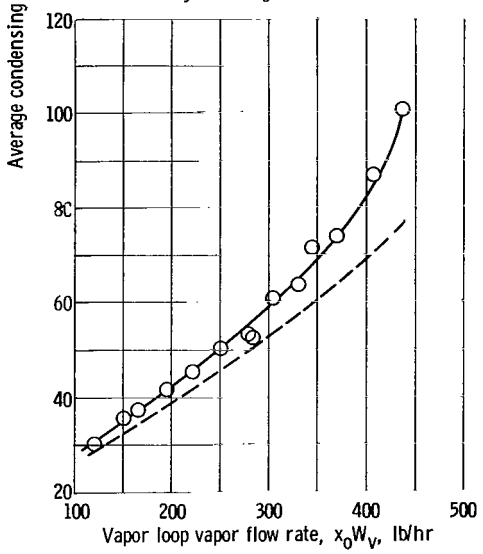

(b) Inventory 2 (1.40 gal). Runs 285 to 298.

Figure 13. - Comparison of calculated and measured condensing length for fixed inventory experiments.

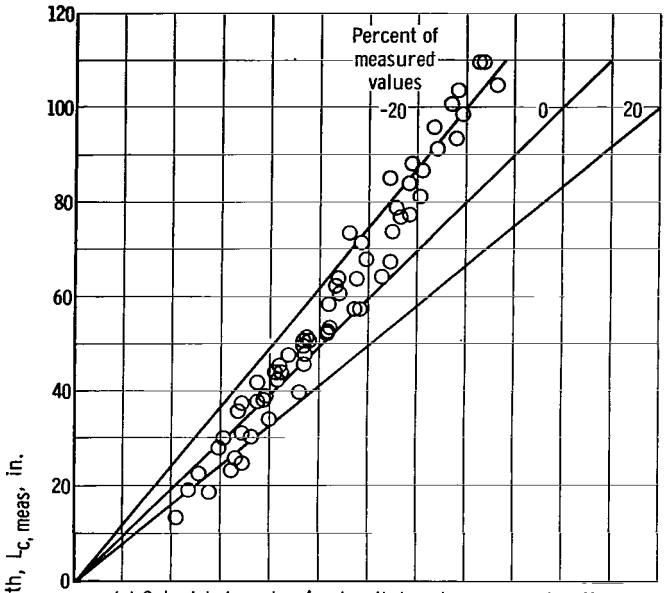

(a) Calculated condensing length based on vapor saturation temperature at outlet equal to saturation temperature at inlet, $T_{SAT,2} = T_{SAT,1}$.

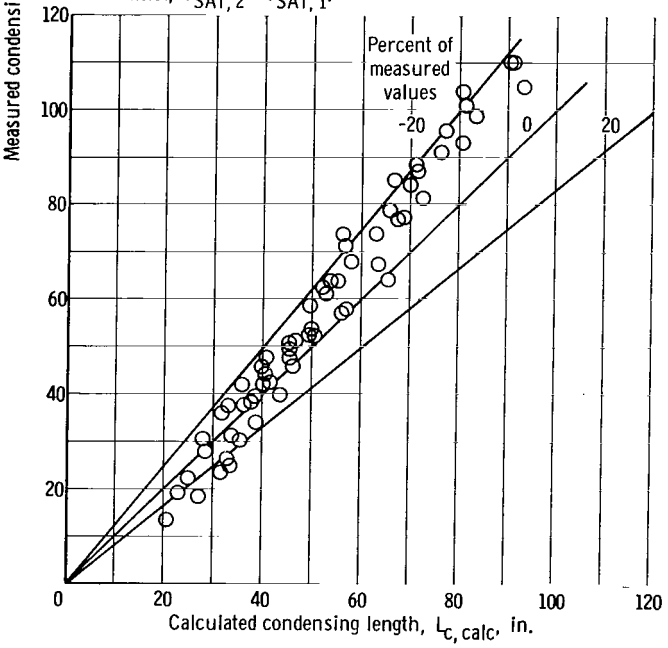

(b) Calculated condensing length based on measured saturation temperature at outlet.

Figure 14. - Comparison of measured and calculated condensing lengths for all runs (see table I).

tory 1 (fig. 13(a)) are within 43 to -20 percent of the values on the curve drawn through the measured data, and the predicted values for inventory 2 (fig. 13(b)) are from 8 to 24 percent lower than the values on the curve faired through the measured data.

Again, as in the comparison of the overall heat-transfer coefficients, the comparison of the condensing lengths for inventory 1 is not quite the same as for inventory 2. This would be expected, however, because of the close relation between the condensing lengths and these overall coefficients. As noted in the discussion on $U_{i,c,meas}$, the characteristics of the measured condensing lengths for the fixed inventory 1 experiments were slightly different from those for the fixed inventory 2 experiments.

The comparison of $L_{c,calc}$ with $L_{c,meas}$ for all runs is presented in figure 14. All values of $L_{c,meas}$ were the average of tubes A and B. In figure 14(a), the condensing length was calculated, as stated in the ANALYTICAL METHODS section, for a constant saturation temperature ($T_{SAT,2} = T_{SAT,1}$). Calculations of condensing length were also made for the actual measured vapor temperature at the interface $T_{SAT,2}$ in order to demonstrate the effect of the vapor temperature drop. As the vapor temperature drop became larger, the temperature difference between the vapor and the coolant became smaller, which caused an increase in the calculated value of the condensing length. At the short condensing lengths, the temperature drops were small, and the differences between the two calculated values of condensing length were negligible. At the longer condensing lengths, however, the temperature drops were larger, due to larger pressure drops, and the differences between the two values of calculated condensing length became noticeable. A plot of the comparison of measured and calculated condensing length based on measured $T_{SAT,2}$ is shown in figure 14(b). A somewhat better comparison to the experimental data is obtained at the larger lengths by including the effects of vapor temperature drop.

Lines representing deviations of ±20 percent from the measured values are also shown on figure 14. It can be seen that almost all the calculated values are within ±20 percent of the measured data and that, in general, the calculated condensing lengths tend to be less than the measured values.

Overall Pressure Drop

The predicted overall pressure drop $\Delta P_{c,calc}$ was calculated by using equations (20) to (27). The two-phase friction drop (ΔP_{TPF}) was calculated from equations (24) or (26), depending upon the flow regime as determined by the Reynolds number of the liquid phase. The vapor phase was always considered to be turbulent (see table I, p. 7). The superficial Reynolds number (ref. 6) of the liquid was calculated at the tube inlet and outlet, and the average value was used to determine the flow regime. The two-phase friction

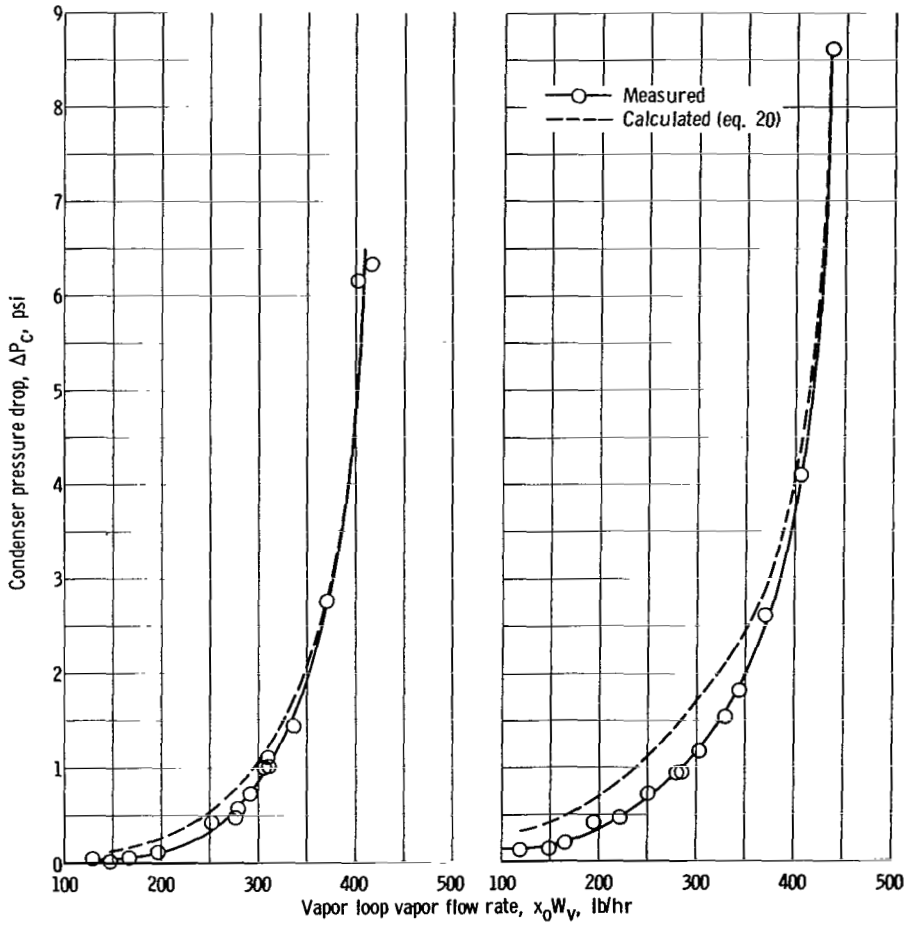

(a) Inventory 1 (1.55 gal). Runs 266 to 283. (b) Inventory 2 (1.40 gal). Runs 285 to 298.

Figure 15. - Comparison of calculated pressure drop, based on measured condensing length, with measured value for fixed inventory experiments.

drop ΔP_{TPF} was calculated by using both the measured and the calculated values of condensing length $L_{c,\,meas}$ and $L_{c,\,calc}$. The measured data $L_{c,\,meas}$ was used in order to obtain a better evaluation of the approximation equations (eqs. (24) and (26)), and the predicted values $L_{c,\,calc}$ were used in order to present an all-calculated pressure drop for comparison. Obviously, the accuracy of the predicted pressure drop $\Delta P_{c,\,calc}$ would be affected by the accuracy of the value used for the condensing length. The comparisons of the measured and calculated pressure drops $\Delta P_{c,\,meas}$ and $\Delta P_{c,\,calc}$ are presented first for the $\Delta P_{c,\,calc}$, computed with $L_{c,\,meas}$ (figs. 15 and 16), and then for the $\Delta P_{c,\,calc}$, computed with $L_{c,\,calc}$ (fig. 17).

The comparison of $\Delta P_{c,\,calc}$ (based on $L_{c,\,meas}$) with $\Delta P_{c,\,meas}$ for the two fixed inventories (inventories 1 and 2) is shown in figures 15(a) and (b). Although the percentage differences are very high (100 percent) at the lower pressure drops, most of the calculated values are within 0.5 pounds per square inch differential of the measured data.

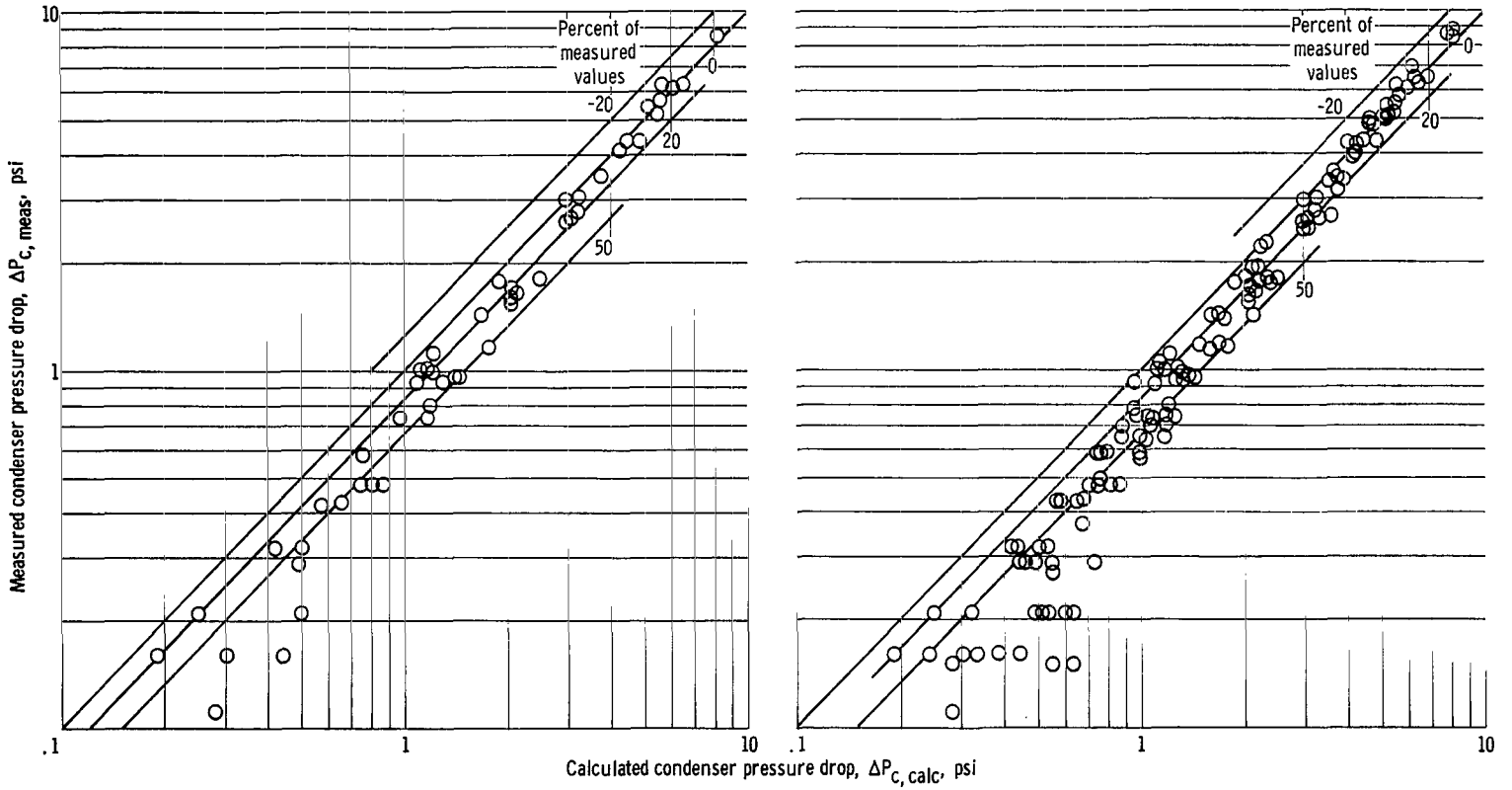

(a) All runs in table I.

(b) Facility runs 99 to 298.

Figure 16. - Comparison of calculated pressure drop, based on the measured condensing length, with the measured values for both fixed and variable inventory experiments.

It should be noted that the predicted values tend to be conservative (i. e., higher than the measured values). Again, the comparison of the inventory 1 data is not the same as for the inventory 2 data. As mentioned previously, in the discussion of $U_{i,c,meas}$, the characteristics of the measured condensing lengths for the fixed inventory 1 experiments were slightly different from those of the fixed inventory 2 experiments.

The comparison of $\Delta P_{c,calc}$ (based on $L_{c,meas}$) with $\Delta P_{c,meas}$ for all runs is presented in figures 16(a) and (b). The data in figure 16(a) are only from the condenser runs listed in table I (p. 7), while the data in figure 16(b) are from the condenser runs in table I plus some additional facility runs that are not tabulated. It can be seen that the predicted values of $\Delta P_{c,calc}$ are high (conservative) at the lower pressure drops (up to about 3 psid) and tend to be low at the higher pressure drops. Lines representing deviations of ±20 and 50 percent from the measured value are shown in figure 16. Therefore, the fact that the Lockhart-Martinelli correlation of φ_g^2 with X^2 showed a data scatter of about ±45 percent in reference 6 indicates that the use of the approximating equations to calculate ΔP_{TPF} results in reasonable values for predicted overall condenser pressure drops greater than about 2 pounds per square inch differential for this condenser. There is considerable scatter at the low pressure drops, which is to be expected since instrumentation error becomes more significant at the lower pressure drops, both in the meas-

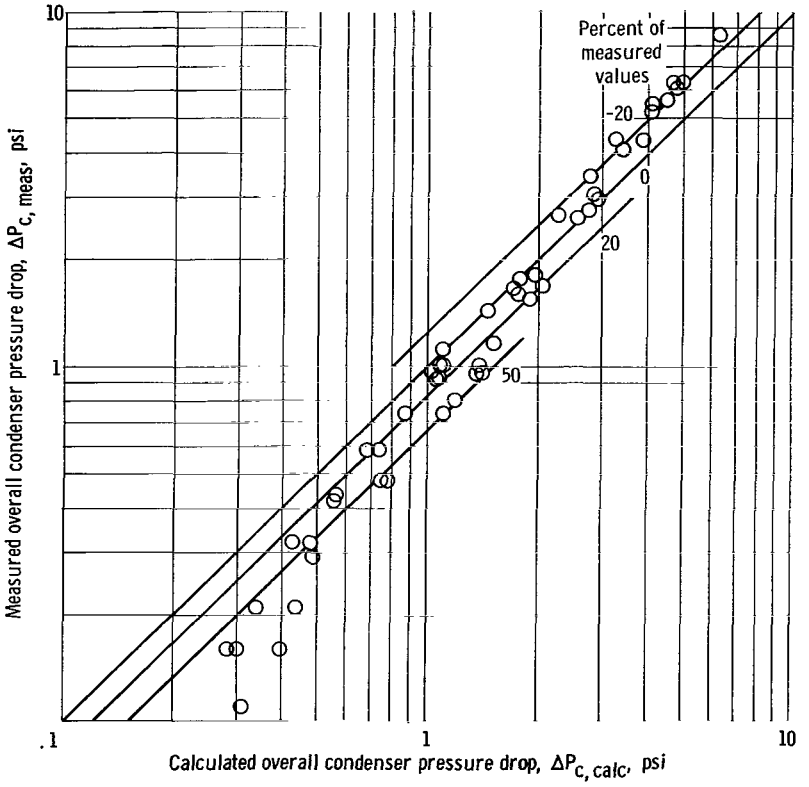

Figure 17. - Comparison of measured condenser pressure drop with predicted pressure drop based on calculated condensing length. All runs in table I.

urement of the pressure drop itself and in the determination of the condensing length. Also, the actual flow distribution (among the 19 tubes) is unknown; therefore, particularly at small flows, it is possible that some of the tubes had more vapor flow than others. The flow distribution could not be detected since only two tubes were instrumented.

The comparison of $\Delta P_{c,calc}$ (based on $L_{c,calc}$) with $\Delta P_{c,meas}$ for all tabulated runs is presented in figure 17. Again, the calculated values are high at the low pressure drops and low at the high pressure drops, when compared with the measured data.

The pressure drop values predicted by using $L_{c,calc}$, however, tend to be lower than the respective values calculated by using $L_{c,meas}$ (fig. 16(a)). This would be expected, since $L_{c,calc}$ tended to be less than $L_{c,meas}$.

CONCLUDING REMARKS

The equations used to calculate the overall heat-transfer coefficient $U_{i,c,calc}$ predicted values that were mostly within ±20 percent of the measured values, with the majority of the calculated values being from 0 to 20 percent higher than the measured values. Measured condenser inlet conditions were used in the calculations.

The predicted values of condensing length were almost all within ±20 percent of the experimental data, with the calculated values tending to be less than the measured values.

The predicted values of overall pressure drop, calculated using both the calculated and measured values of condensing lengths, were mostly within 50 to -20 percent of the experimental data, with the largest percent deviations at the small pressure drops. The calculated values of the overall condenser pressure drop tended to be conservative (i. e., higher than the actual measured values) although the values predicted with $L_{c,calc}$ were, in general, smaller than the corresponding values calculated with $L_{c,meas}$.

Lewis Research Center,
National Aeronautics and Space Administration,
Cleveland, Ohio, July 5, 1966,
120-27-04-02-22.

APPENDIX A

SYMBOLS

A_{hi}	heat-transfer area, based on tube inside diameter, sq ft
A_i	total flow area, based on the tube inside diameter, sq ft
A_s	coolant flow area, sq ft
C_p	specific heat, Btu/lb
D_E	equivalent diameter of condenser shell, ft
D_i	tube inside diameter, ft
D_o	tube outside diameter, ft
D_s	condenser inner shell inside diameter, ft
f	friction factor
G_c	coolant mass velocity, $\frac{W_c}{A_s}$, lb/(hr)(sq ft)
G_f	vapor mass velocity at tube outlet, $\frac{xW_v}{A_i}$, lb/(hr)(sq ft)
G_m	mean vapor mass velocity, 0.58 G_o lb/(hr)(sq ft)
G_o	vapor mass velocity at tube inlet, $\frac{x_o W_v}{A_i}$, lb/(hr)(sq ft)
g_c	conversion factor, 4.18×10^8 (lb mass/lb force)(ft/hr)/hr
h_{fg}	enthalpy of vaporization, Btu/lb
h_i	film coefficient of heat transfer on inside of tube, Btu/(hr)(sq ft)(^oF)
h_o	film coefficient of heat transfer on outside of tubes, Btu/(hr)(sq ft)(^oF)
K_T	quality dependent factor in turbulent-turbulent two-phase friction pressure drop equation
K_V	quality dependent factor in viscous-turbulent two-phase friction pressure drop equation
k	thermal conductivity, Btu/(hr)(sq ft)(^oF)/ft
L	length, ft
N	number of tubes
N_{Gr}	Grashof number
N_{Pr}	Prandtl number
N_{Re}	Reynolds number
P	pressure, lb/sq ft
P_{C2C}	pressure of coolant at condenser outlet, psia
P_{H1B}	pressure of heating fluid at boiler inlet, psia
P_{V1B}	pressure of vapor loop fluid at boiler inlet, psia

P_{V1C}	pressure of vapor loop fluid at condenser inlet, psia
P_w	wetted perimeter, ft
ΔP	pressure drop, lb/sq ft
ΔP_E	pressure change at tube inlet, lb/sq ft
ΔP_H	pressure loss from inlet piping to inlet vapor plenum, lb/sq ft
ΔP_M	pressure change due to momentum recovery, lb/sq ft
ΔP_{TPF}	two-phase friction pressure loss, lb/sq ft
Q	heat load, Btu/hr
S	axial coolant temperature, ^oF
S_i	heat-transfer area per unit length, based on tube inside diameter, sq ft/ft
S_m	heat-transfer area per unit length, based on mean tube diameter, sq ft/ft
S_o	heat-transfer area per unit length, based on tube outside diameter, sq ft/ft
T	axial vapor temperature, ^oF
T_{CI}	coolant temperature at end of condensing length, ^oF
T_{C1C}	coolant temperature at condenser inlet, ^oF
T_{C2C}	coolant temperature at condenser outlet, ^oF
T_{H1B}	temperature of heating loop fluid at boiler inlet, ^oF
T_{H2B}	temperature of heating loop fluid at boiler outlet, ^oF
$T_{SAT,1}$	vapor saturation temperature at tube inlet, ^oF
$T_{SAT,2}$	vapor saturation temperature at end of condensing length, ^oF
T_{V1B}	temperature of vapor loop fluid at boiler inlet, ^oF
T_{V2B}	temperature of vapor loop fluid at boiler outlet, ^oF
T_{V1C}	temperature of vapor loop fluid at condenser inlet, ^oF
T_{V2C}	temperature of vapor loop fluid at condenser outlet, ^oF
ΔT_{cc}	directly measured temperature change of coolant from inlet to outlet of condenser, ^oF
ΔT_{HB}	directly measured temperature change of heating loop fluid from inlet to outlet of boiler, ^oF
ΔT_{LM}	log-mean temperature difference
t	tube wall thickness, ft
U_i	overall heat-transfer coefficient, based on tube inside area, Btu/(hr)(sq ft)(^oF)
V	velocity, ft/hr
W	flow, lb/hr
W_A	axial wall temperature of tube A, ^oF
W_B	axial wall temperature of tube B, ^oF

W_c	coolant flow, lb/hr
X	Lockhart-Martinelli parameter, $\sqrt{\frac{(\Delta P/L)_\ell}{(\Delta P/L)_g}}$
x	vapor quality, $\frac{W_g}{W_v}$
x_o	vapor quality at condenser inlet
Y/L	fraction of condensing length
α_T	quality dependent factor in turbulent two-phase friction pressure drop equation
α_V	quality dependent factor in viscous two-phase friction pressure drop equation
β_T	temperature dependent properties factor in turbulent two-phase friction pressure drop equation
β_V	temperature dependent properties factor in viscous two-phase friction pressure drop equation
μ	viscosity, lb/(ft)(hr)
ρ	density, lb/cu ft
φ_g	Lockhart-Martinelli parameter, a function of X

Subscripts:

A	condenser tube A (at the top)
B	condenser tube B (at the bottom)
b	evaluated at bulk temperature of liquid
c	condensing, condensing portion of heat exchanger
calc	calculated value
g	gas or vapor
H	heating loop
ℓ	liquid
meas	measured value
o	tube inlet
p	pipe
sc	subcooler, subcooling portion
TPF	two-phase friction
TT	turbulent-liquid - turbulent-gas regime
t	tube
v	vapor loop
VT	viscous-liquid - turbulent-gas regime
w	wall or evaluated at wall temperature
1, 2, . . .	sequence

APPENDIX B

CONDENSER DESIGN CONSIDERATIONS

The requirements and considerations used in the design of the condenser in this test facility are presented in the following paragraphs.

General Requirements

The requirements established for this condenser were as follows:

(1) The heat rejection rate would be a nominal 500 000 Btu per hour, which was approximately the same as that of the alkali metal facility (see INTRODUCTION).

(2) The unit should be horizontal and contain small diameter tubes in order to reduce the effects of gravity.

(3) The unit must be less than 10 feet long to permit disassembly. It was decided that the condenser should be a multitube, shell-and-tube type with triangular pitch so that the unit would be small and simple.

Operating Range

An operating range of about 5 to 25 pounds per square inch absolute was chosen. In this range, the properties of water were comparable with those of potassium in the operating range of the alkali metal facility. A nominal maximum flow rate of 500 pounds per hour was established.

Tube Size and Number of Tubes

Tubes of nominal 0.25-inch inside diameter with a 0.035-inch wall thickness were used. In order to efficiently fill a shell of circular cross section, the following number of tubes were considered: N = 7, 13, 19, 31, or 55. Therefore, in order to determine which number of tubes should be used, various condenser characteristics were calculated for several values of N, as discussed in the following paragraphs.

Vapor velocity. - The maximum velocity of the vapor is plotted against the number of tubes in figure 18 for the maximum flow rate of 500 pounds per hour at several values of saturation pressure. From this figure, it was decided that the maximum flow rate

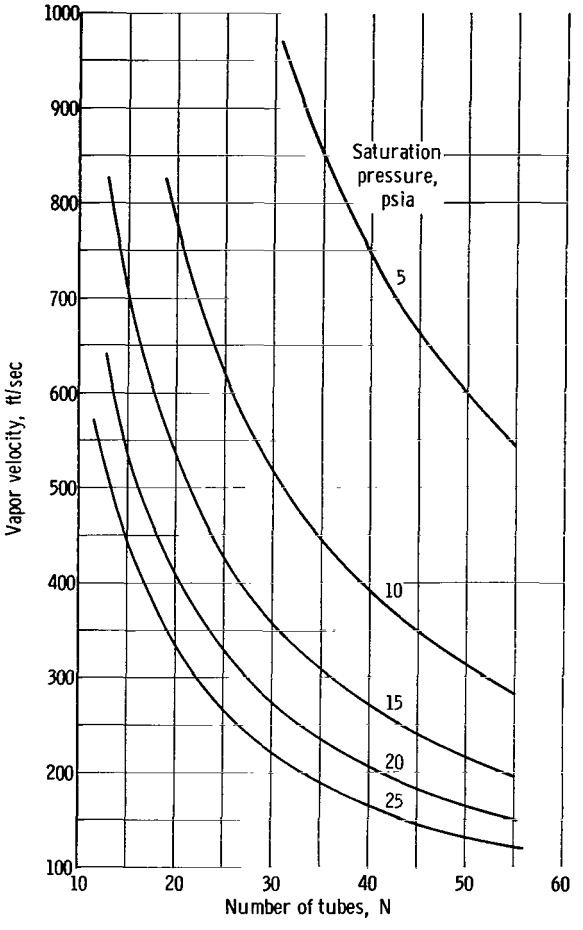

Figure 18. - Vapor velocity against number of tubes with total vapor flow of 500 pounds per hour for several values of saturation pressure.

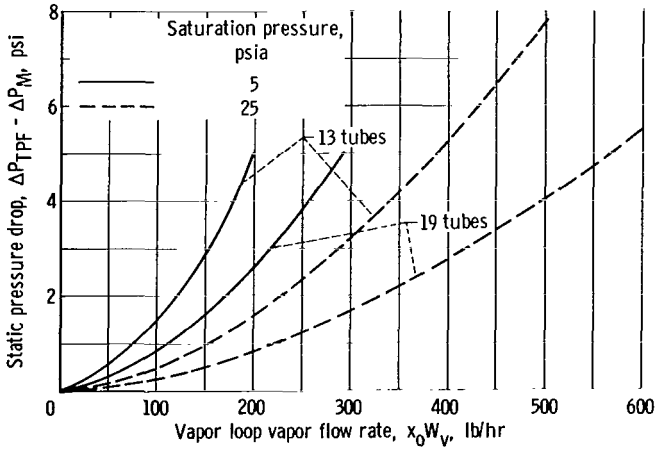

Figure 19. - Static pressure drop in tubes with condensing length of 10 feet for two values of saturation pressure.

could seldom be achieved with less than 13 tubes and that the vapor velocities at the higher pressures would be too low with 31 or more tubes. Therefore, either 13 or 19 tubes was preferable, provided that the pressure drops were reasonable and the heat-transfer area was adequate.

Tube pressure drop. - The next consideration was the pressure drop in the tubes. The two-phase friction drop ΔP_{TPF} and the momentum recovery ΔP_M were calculated for a condensing length of 10 feet by using equations (25) and (27) in the text and by assuming a 100 percent quality of vapor at the tube inlet. The static pressure drop $\Delta P_{TPF} - \Delta P_M$ results are as shown in figure 19. It is apparent from the figure that (1) a full flow rate of 500 pounds per hour cannot be attained with a condensing length of 10 feet for a saturation pressure of 5 pounds per square inch absolute, (2) for any given flow rate and saturation pressure, the 19 tube configuration would have a smaller pressure drop, and (3) for any given flow rate and pressure drop, the 19 tube configuration would permit operation at a lower saturation pressure.

Heat-transfer area. - Since the maximum condenser length was limited to 10 feet, it was apparent that 19 tubes would provide more surface area than 13 tubes, and therefore would permit a lower minimum heat flux $Q_c/A_{hi,c}$ for any given condensing heat load Q_c. The heat-transfer area of either 13 or 19 tubes would be adequate if the overall heat-transfer coefficient $U_{i,c}$ is large

enough for the range of log-mean temperature difference ΔT_{LM} available from the facility.

Therefore, since the use of 19 tubes would require a smaller $U_{i,c}$, or permit operation at a lower ΔT_{LM}, and would result in reasonable pressure drops and permit maximum flow rate operation at a lower saturation pressure, it was decided that 19 tubes would be used.

Final Considerations

A tube spacing of 1/8 inch was used to allow the tube entrances to be slightly rounded. This dimension determined the shell size. The overall heat-transfer coefficient $U_{i,c}$ was then checked by using equation (7) and was found to be large enough that the heat-transfer area of 19 tubes was adequate.

APPENDIX C

DERIVATION OF APPROXIMATING EQUATIONS FOR TWO-PHASE FRICTION PRESSURE DROP DURING CONDENSATION

The derivation of the equations used to calculate the two-phase friction pressure drop during condensation, based on the Lockhart-Martinelli (ref. 6) correlation for two-phase, two-component flow, is presented herein. These equations are derived in a manner similar to that used in reference 7 by substituting an approximating equation for the Lockhart-Martinelli correlation of φ_g against X and by integrating the various parameters involved over the condensing length of the condenser.

The Lockhart-Martinelli correlation was of the form

$$\left(\frac{dP}{dL}\right)_{TPF} = \varphi_g^2 \left(\frac{dP}{dL}\right)_g \tag{C1}$$

where

$$\varphi_g = f(X)$$

and

$$X^2 = \frac{\left(\frac{dP}{dL}\right)_\ell}{\left(\frac{dP}{dL}\right)_g} \tag{C2}$$

For the viscous-liquid - turbulent-gas regime $\left(\left(N_{Re}\right)_{\ell,t} < 1000,\ \left(N_{Re}\right)_{g,t} > 2000\right)$ for each phase flowing alone

$$\left(\frac{dP}{dL}\right)_\ell = \frac{32 V_{\ell,t} \mu_\ell}{g_c D_i^2} \tag{C3}$$

$$\left(\frac{dP}{dL}\right)_g = \frac{2f V_{g,t}^2 \rho_g}{g_c D_i} \tag{C4}$$

where

$$f = \frac{0.046}{\left(N_{Re}\right)_{g,t}^{0.2}} \tag{C5}$$

The superficial local velocities are defined as

$$V_{\ell,t} = \frac{W_\ell}{\rho_\ell A_i} \tag{C6}$$

$$V_{g,t} = \frac{W_g}{\rho_g A_i} \tag{C7}$$

Combining equations (C2) to (C7),

$$X_{VT}^2 = \frac{32}{0.092} \frac{W_\ell}{W_g} \frac{\rho_g}{\rho_\ell} \frac{\mu_\ell}{\mu_g} \left(N_{Re}\right)_{g,t}^{-0.8} \tag{C8}$$

In a condenser, the values of Reynolds numbers, flow rates, and velocities change continuously over the length of the condenser; therefore, local values must be used. The fluid properties are evaluated at the condenser inlet static pressure and are assumed constant. Assuming $Q_c/A_{hi,c}$ is constant,

$$W_g = W_{g,o}\left(1 - \frac{Y}{L}\right) \quad \left(\text{where } W_{g,o} = x_o W_v\right) \tag{C9}$$

$$W_\ell = W_v - W_g \tag{C10}$$

$$\left(N_{Re}\right)_{g,t} = \left(N_{Re}\right)_{g,o}\left(1 - \frac{Y}{L}\right) \tag{C11}$$

$$V_{g,t} = V_{g,o}\left(1 - \frac{Y}{L}\right) \tag{C12}$$

and

$$\frac{W_\ell}{W_g} = \frac{1 - x_o\left(1 - \frac{Y}{L}\right)}{x_o\left(1 - \frac{Y}{L}\right)} \tag{C13}$$

Combining equations (C8), (C11), and (C13), and taking the square root,

$$X_{VT} = 18.65\left(N_{Re}\right)_{g,o}^{-0.4}\left(1 - \frac{Y}{L}\right)^{-0.4}\left[\frac{1 - x_o\left(1 - \frac{Y}{L}\right)}{x_o\left(1 - \frac{Y}{L}\right)}\right]^{0.5}\left[\frac{\rho_g \mu_\ell}{\rho_\ell \mu_g}\right]^{0.5} \tag{C14}$$

The Lockhart-Martinelli viscous-liquid - turbulent-gas regime curve of φ_g against X was approximated over the range of interest for a condenser (the value of X is very low over most of the condensing length) by the relation

$$\varphi_{g_{VT}} = 2.2X_{VT}^{0.13} \tag{C15}$$

Combining equations (C4), (C5), (C11), and (C12) yields

$$\left(\frac{dP}{dL}\right)_g = \frac{0.092\rho_g V_{g,o}^2}{g_c D_i}\left(1 - \frac{Y}{L}\right)^{1.8}\left(N_{Re}\right)_{g,o}^{-0.2} \tag{C16}$$

Combining equations (C1), (C14), (C15), and (C16) and integrating yield

$$\frac{\left(\Delta P_{TPF}\right)_{VT}}{L_c} = \frac{0.954}{x_o^{0.13}}\frac{\rho_g V_{g,o}^2}{g_c D_i}\left(\frac{\rho_g \mu_\ell}{\rho_\ell \mu_g}\right)^{0.13}\left(N_{Re}\right)_{g,o}^{-0.304}$$

$$\times \int_0^1 \left[1 - x_o\left(1 - \frac{Y}{L}\right)\right]^{0.13}\left(1 - \frac{Y}{L}\right)^{1.566} d\left(\frac{Y}{L}\right) \tag{C17}$$

When the integral is evaluated, the result is a power series of x_o. By selecting values

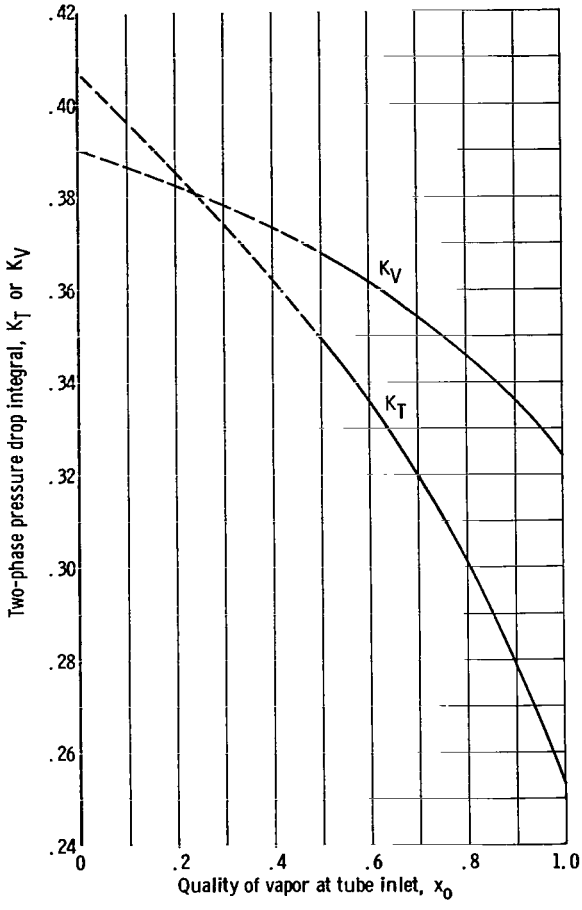

Figure 20. - Two-phase friction pressure drop integral as a function of inlet vapor quality. Dashed portions of curves denote extrapolation.

for x_o, the value of the integral can be plotted as a function of x_o, as in figure 20, and is defined as K_V. The equation for the viscous-turbulent regime two-phase friction condensing pressure drop then becomes

$$\left(\Delta P_{TPF}\right)_{VT} = \frac{0.954}{x_o^{0.13}} \frac{\rho_g V_{g,o}^2}{g_c D_i} \times \left(\frac{\rho_g \mu_\ell}{\rho_\ell \mu_g}\right)^{0.13} \left(N_{Re}\right)_{g,o}^{-0.304} K_V L_c \qquad \text{(C18)}$$

Further reduction of this equation is possible, however, by grouping the temperature dependent properties, the quality dependent coefficients, and the physical constants. Substitution of

$$A_i = \frac{N\pi D_i^2}{4} \qquad \text{(C19)}$$

$$V_{g,o} = \frac{x_o W_v}{\rho_g A_i} \qquad \text{(C20)}$$

and

$$\left(N_{Re}\right)_{g,o} = \frac{D_i G_o}{\mu_g} = \frac{D_i x_o W_v}{\mu_g A_i} \qquad \text{(C21)}$$

into equation (C18) yields

$$\left(\Delta P_{TPF}\right)_{VT} = 1.433\, x_o^{1.566} \left(\frac{\mu_\ell}{\rho_\ell}\right)^{0.13} \frac{\mu_g^{0.174}}{\rho_g^{0.87} g_c} \frac{W_v^{1.696}}{N^{1.696} D_i^{4.696}} K_V L_c \qquad \text{(C22)}$$

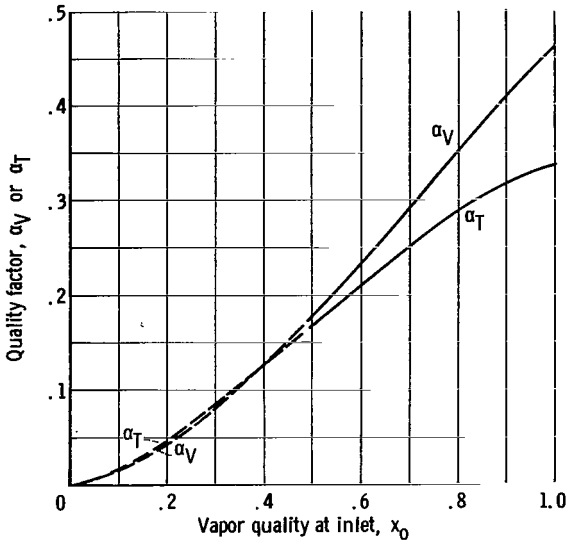

Figure 21. - Quality-dependent factor in two-phase friction pressure drop equation. Dashed portions of curves denote extrapolation.

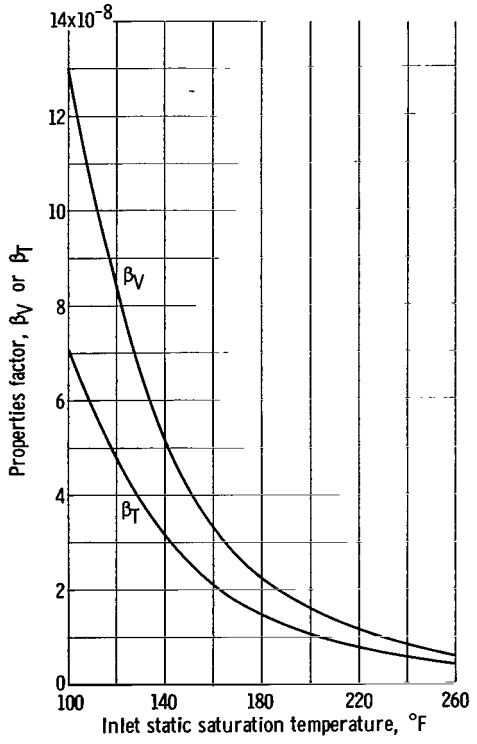

Figure 22. - Values of factors β_V and β_T for water used in two-phase friction pressure drop equation.

Defining

$$\alpha_V = 1.433\, K_V x_o^{1.566} \qquad \text{(C23)}$$

and

$$\beta_V = \left(\frac{\mu_\ell}{\rho_\ell}\right)^{0.13} \frac{\mu_g^{0.174}}{\rho_g^{0.87} g_c} \qquad \text{(C24)}$$

gives the following for equation (C22):

$$\left(\Delta P_{TPF}\right)_{VT} = \frac{\alpha_V \beta_V W_v^{1.696}}{N^{1.696} D_i^{4.696}} L_c \qquad \text{(C25)}$$

or, for simplicity,

$$\left(\Delta P_{TPF}\right)_{VT} = \frac{\alpha_V \beta_V W_v^{1.7}}{N^{1.7} D_i^{4.7}} L_c$$

Again, equation (C23) can be evaluated and α_V plotted against x_o by selecting values for x_o, as in figure 21. For any given fluid, equation (C24) can be evaluated and β_V plotted against temperature, as in figure 22 for water. The property data for figure 22 were taken from references 4 and 8.

For the turbulent-liquid - turbulent-gas regime, the use of the same procedure, with the Lockhart-Martinelli turbulent-liquid - turbulent-gas regime curve of φ_g against X approximated over the range of interest by the relation

$$\left(\varphi_g\right)_{TT} = 3.05 X_{TT}^{0.19} \qquad \text{(C26)}$$

yields the following equation:

$$\left(\Delta P_{TPF}\right)_{TT} = \frac{\alpha_T \beta_T W_v^{1.8}}{N^{1.8} D_i^{4.8}} \tag{C27}$$

where

$$\alpha_T = 1.328\, K_T x_o^{1.46} \tag{C28}$$

and

$$\beta_T = \frac{\mu_\ell^{0.038}}{\rho_\ell^{0.19}} \frac{\mu_g^{0.162}}{\rho_g^{0.81} g_c} \tag{C29}$$

with

$$K_T = \int_0^1 \left[1 - x_o\left(1 - \frac{Y}{L}\right)\right]^{0.34} \left(1 - \frac{Y}{L}\right)^{1.46} d\left(\frac{Y}{L}\right) \tag{C30}$$

The coefficient K_T is a function of inlet vapor quality x_o and is shown in figure 20. Values of α_T are shown in figure 21 and values of β_T for water are shown in figure 22.

REFERENCES

1. Zipkin, Morris A.; and Edwards, Russell N., eds.: Power Systems for Space Flight. Vol. 11 of Progress in Astronautics and Aeronautics, Martin Summerfield, ed., Academic Press, 1963.

2. Fenn, David B.; Coe, Harold H.; and Gutierrez, Orlando A.: Steady-State Performance of a Modified Rankine Cycle System Using Water. NASA TN D-3333, 1966.

3. Carpenter, E. F.; and Colburn, A. P.: The Effect of Vapor Velocity on Condensation Inside Tubes. Proceedings of the General Discussion on Heat Transfer, Inst. Mech. Eng., (London), and ASME, 1951, pp. 20-26.

4. McAdams, William H.: Heat Transmission. Third ed., McGraw-Hill Book Co., Inc., 1954.

5. Anon.: Flow of Fluids Through Valves, Fittings, and Pipes. Tech. Paper No. 409, The Crane Co., Chicago, Ill., May 1942.

6. Lockhart, R. W.; and Martinelli, R. C.: Proposed Correlation of Data for Isothermal Two-Phase, Two Component Flow in Pipes. Chem. Eng. Prog., vol. 45, no. 1, Jan. 1949, pp. 39-48.

7. Coombs, M. G.; Stone, R. A.; and Kapus, T.: The SNAP 2 Radiative Condenser Analysis. Rep. No. NAA-SR-5317, Atomics International, 1960.

8. Keenan, Joseph H.; and Keyes, Frederick G.: Thermodynamic Properties of Steam. John Wiley and Sons, Inc. 1936. (28th printing, 1955.)

NASA-Langley, 1966 E-3229

"The aeronautical and space activities of the United States shall be conducted so as to contribute . . . to the expansion of human knowledge of phenomena in the atmosphere and space. The Administration shall provide for the widest practicable and appropriate dissemination of information concerning its activities and the results thereof."

—NATIONAL AERONAUTICS AND SPACE ACT OF 1958

NASA SCIENTIFIC AND TECHNICAL PUBLICATIONS

TECHNICAL REPORTS: Scientific and technical information considered important, complete, and a lasting contribution to existing knowledge.

TECHNICAL NOTES: Information less broad in scope but nevertheless of importance as a contribution to existing knowledge.

TECHNICAL MEMORANDUMS: Information receiving limited distribution because of preliminary data, security classification, or other reasons.

CONTRACTOR REPORTS: Technical information generated in connection with a NASA contract or grant and released under NASA auspices.

TECHNICAL TRANSLATIONS: Information published in a foreign language considered to merit NASA distribution in English.

TECHNICAL REPRINTS: Information derived from NASA activities and initially published in the form of journal articles.

SPECIAL PUBLICATIONS: Information derived from or of value to NASA activities but not necessarily reporting the results of individual NASA-programmed scientific efforts. Publications include conference proceedings, monographs, data compilations, handbooks, sourcebooks, and special bibliographies.

Details on the availability of these publications may be obtained from:

SCIENTIFIC AND TECHNICAL INFORMATION DIVISION

NATIONAL AERONAUTICS AND SPACE ADMINISTRATION

Washington, D.C. 20546